UNIVERSITÀ DEGLI STUDI DI NAPOLI FEDERICO II

DOTTORATO DI RICERCA IN
TERAPIE AVANZATE BIOMEDICHE E CHIRURGICHE
XXXIII CICLO

Coordinatore Prof. Giovanni Di Minno

TESI DI DOTTORATO

"Thyroid Hormone Acts as a Master Regulator of Quiescence and Self-Renewal in Stem Cells"

Relatore
Ch.mo prof.ssa Monica Dentice

Candidato
Maria Angela De Stefano

Index

1. Summary

Stem cells are critical for the regeneration and homeostasis of adult tissues. Thyroid hormone (TH), whose intracellular concentration is regulated by deiodinases (D2 and D3), is implicated in stem cell function and lineage progression. The aim of this study was to determine the role of TH and its intracellular metabolism in stem cell quiescence, which is still a poorly understood condition. Here we show that D2 expression marks quiescent stem cells in muscle and skin. Acute D2-depletion in quiescent muscle stem cells triggers their spontaneous transition from G_0 into a G_{Alert} state. Upon muscle injury, D2-depletion increases the proliferative potential of activated precursor cells but impairs self-renewal of progenitors returning to quiescence. Genetic D2-depletion leads, in the long run or upon multiple injuries, to depletion of the stem cell pool and regenerative failure. Mechanistically, D2-produced TH sustains Notch signalling by directly promoting the expression of Notch receptors and their canonical target genes. In normal and pathological settings, transient drug-induced D2 blocking accelerates muscle regeneration and skin wound healing. In conclusion, a D2-induced increased intracellular TH concentration is critical in maintaining stem cell quiescence and in regulating self-renewal. In this context, tissue-specific manipulation of TH may be an innovative therapeutic tool in the field of regenerative medicine.

2. Background

2.1 Skeletal Muscle Stem Cells (MuSCs)

Stem cells sustain continuous tissue homeostasis by generating tissue progeny while self-renewing through cell division (1, 2). This process is necessary to ensure continuous tissue maintenance in various organs, and most of the stem cell properties, such as quiescence, self-renewal, and differentiation are controlled by the stem cell microenvironment, also known as the "niche" (3-6). Under normal conditions, adult stem cells in most tissues are mitotically quiescent in a state required to preserve stem cell function (G_0 phase), from which they can rapidly exit in response to various stimuli (stress, injury or tissue homeostasis). Upon activation, most of the stem cell progeny undergoes terminal differentiation, while a subset of stem cells exits from the cell cycle and returns to a quiescent state thereby re-establishing the stem cell pool in terms of number and tissue regenerative capacity (7).

Significant progress has been made toward elucidating the signals involved in the regulation of adult stem cells and tissue homeostasis (6). Among other important functions, it is now well established that Notch signalling pathway plays a role in maintaining stem cells of different tissues in a quiescent state (8). In particular, Notch signalling is crucial in the control of stem cells by also exerting its action in the self-renewal process (9). The activation of Notch results in the translocation to the nucleus of its intracellular domain, which interacts with CSL/RBP-J transcription factor thereby activating target genes, such as the Hey and Hes gene families (10). Despite significant progress, the precise molecular mechanisms governing the quiescent state of stem cells are poorly understood. In this context, a relevant discovery was achieved by the identification of an intermediate state between G_0 and G1 phase of the cell cycle, designated "G_{Alert}" in which stem cells are more rapidly poised to enter the cell cycle in response to injury (11). This phase is induced by the circulating Hepatocyte Growth Factor activator released by different injuries (12).

2.2 Intracellular Thyroid hormone metabolism

The intracellular thyroid hormone concentration is regulated by synergicaction of membrane transporters, deiodinase and TH nuclear receptors (13-15). Although thyroid hormones are fat-soluble, their inflow and outflow between cell and blood flow does not occur by simple diffusion but the transporters are used: the monocarboxylate transporter 8 (MCT8), MCT10 and the C1 anionpolypeptide organic (OATP). The iodothyronine deiodinase family consists of three types (D1, 2 and 3), that are expressed in tissue- specific in adulthood and fetal (16) and catalyze activation or inactivation of TH. (13, 17, 18). In particular, D1 and D2 convert pro-hormone thyroxine (T4) to the active hormone T3. Conversely, D3 converts T3 (triiodothyronine) to T2 (diiodothyronine) and T4 to rT3 (reverse triiodothyronine), both inactive thyroid hormone metabolites. D1 is an integral plasma membrana protein and is mainly expressed in the liver, the thyroid and kidney. It converts T4 to T3 primarily to provide T3 for the circulation as well as scavenger enzyme that recycles iodine to replenish the thyroid; iodine reservoir (16, 19). D2 is an endoplasmatic reticulum resident protein and is mainly expressed in muscle, brain, bone and adipose tissue. In contrast with D1, it not affects serum hormone concentrations, and is considered the major TH activator at intracellular level (16). D3 is localized in the plasma membrane and is hightly expressed during embryonic development, while in adult life it is expressed in brain and skin. D3 is major TH inactivating enzyme that protects tissue from TH excess. Canonical action of active TH (T3) is mediated by the interaction of nuclear hormone receptors (TRs) with the promoters of specific target genes, a process that can both activate and repress their transcription. TRs are ligand-activated transcription factors that modulate gene expression through interaction with coactivators, corepressors and association with transcriptional machinery. Several TR isoforms have been identified: TRα and TRβ, located in 2 different chromosomes, encodes for 4 T3-binding isoforms: $\alpha 1$, $\beta 1$, $\beta 2$ e $\beta 3$ (20). The TRs act on specific thyroid hormone response elements (TREs) located on the promoter regions of T3-target genes (20). The expression of TRs is tissue and time-specific, depending on developmental cells stage (21). Moreover, TRs activity is modulated in a T3-dependent fashion by several regulatory proteins (22).

2.3 Role of deiodinases in muscle stem cells proliferation and development.

Modulation of thyroid hormone metabolism is important for development and homeostasis of many tissues, including muscle and skin. In particular, TH plays a key role in proliferation, differentiation, homeostasis and development of skeletal muscle stem cells (MuSCs). The myogenesis process is characterized by the activation of a primary myogenic stem cell population referred to as‘‘satellite cells’’ which give rise to activated proliferating myoblasts or myoblast precursor cells (mpcs), followed by cell differentiation and fusion into regenerated myofibers. We previously showed that the balance between the T3-activating (D2) and inactivating (D3) deiodinases in myoblast precursor cells is necessary for the lineage progression of muscle stem cells (18, 23). Moreover, TH controls the survival pathway of colorectal cancer stem cells affecting Notch levels (24).

2.4 Thyroid hormone and Duchenne Muscular Dystrophy (DMD)

Muscular dystrophies are a genetically and clinically heterogeneous group of muscle disorders that cause progressive weakness and loss of muscle mass. Among muscular dystrophies the most common is Duchenne Muscular Dystrophy (DMD). DMD is a devastating recessive X-linked muscle degenerative disease caused by frame-shift deletions, duplications, or point mutations in the dystrophin (DMD) gene (25, 26). t is a sex-linked disorder, meaning that it strikes males almost exclusively and most females who carry the genetic defect are unaffected, but they have a 50 percent probability of passing the disease to each of their sons. Here, we used the mdx mouse model that is genetically similar to humans with DMD in that muscles in both lack dystrophin. In contrast, the mdx mouse model produces utrophin which is able to substitute the functions of dystrophin by improving the condition of mdx mice. Thyroid hormone is important for muscle cell development and maturation and both fiber size and myosin heavy chain (MHC) expression are under the influence of thyroid status (27). it has been shown that hyperthyroidism in mdx mice appears to increase the amount of dystrophic damage in slow limb muscles and in the heart. This was due to an increased expression of fast MHC isoforms in slow-twitch muscles and increased cardiac work during hyperthyroidism (27, 28).

3.1 Aim of the project

Thyroid Hormone (TH) is a pleotropic agent that regulates crucial biological functions such as normal growth, development and metabolism of nearly all vertebrate tissues. In particular, in skeletal muscle, TH plays a critical role in regulating the function of satellite cells. TH metabolism is dynamically modified during myogenesis and muscle regeneration by two TH-regulator enzymes, Deiodinase D2 and D3. This modulation is essential for proper muscle repair and satellite amplification and differentiation.

However, precise role of the thyroid hormone in quiescent muscle stem cells is still unknown. Aim of this study was to analyse whether and how TH signalling is involved in the control of quiescence. Using inducible genetic systems to ablate *Dio2* gene specifically in stem cells, we demonstrate that TH producing D2 maintains the quiescence state in muscle and skin and regulates stem cell self-renewal. We provide evidence that at least in muscle, this function is achieved through the sustaining of the Notch signalling. Moreover, D2-depletion leads to transition of the dormient-quiescent satellite cell to a G_{Alert} state, which upon injury significantly accelerate the activation of MuSCs and tissue repair. In conclusion, here we describe a novel pathway by which TH metabolism regulates homeostasis, cell self-renewal and regenerative potential in the stem cell compartment in different tissues. This requires a cell-autonomous mechanism able to rapidly modulate intracellular T3 concentration and adapt it to varying metabolic needs occurring in stem cells.

4. RESULTS

4.1 D2 is expressed in quiescent muscle stem cells and is downregulated upon cell activation

We firstly analysed D2 expression within the different subset of muscle stem cells (Pax7-nGFP cells) fractionated into distinct subpopulation based on GFP intensity. D2 expression was highest in Pax7-nGFP^{Hi} cells (the most quiescent Pax7 subgroup) (Figure 1A and (23)). Based on these findings, we speculated that D2 could mark quiescent stem cells. To address this issue, we analysed D2 expression by immunofluorescence in the previously characterized 3xFLAG-D2 knock-in mouse (29). We found that D2 co-localized with the muscle stem cell marker Pax7^{+} (30)in resting tibialis anterior (TA) muscle (Figure 1B). Interestingly, D2 expression was dynamically regulated in muscle stem cells during lineage progression, where D2 staining co-localized with Pax7^{+}cells at early time points in single isolated muscle fiber, and its expression declined with time (Figure 1C). Accordingly, D2 on fibers was not detectable in proliferating cells identified by 5-ethynyl-2′-deoxyuridine (EdU) incorporation assay (Figure 1D and 1E), and its expression was inversely correlated with D3 (a marker of proliferative cells (23)) (Figure 1D and 1E). Accordingly, in freshly isolated stem cells its expression was elevated in quiescent and was dramatically reduced upon proliferation (Figure 1F). Consistent with the D2-mediated increase of intracellular thyroid hormone signaling, we observed that other components of the TH signal machinery, namely the deiodinase D3 (*Dio3*) the *Thra*, *Thrb* receptors and *Mct8*, *Mct10* and *Oatp1c1* transporters were expressed in quiescent muscle stem cells (Figure 1G-M) and appropriately decreased or increased (*Dio3)* as muscle stem cells transited from quiescence to an activation state (Figure 1G-M).

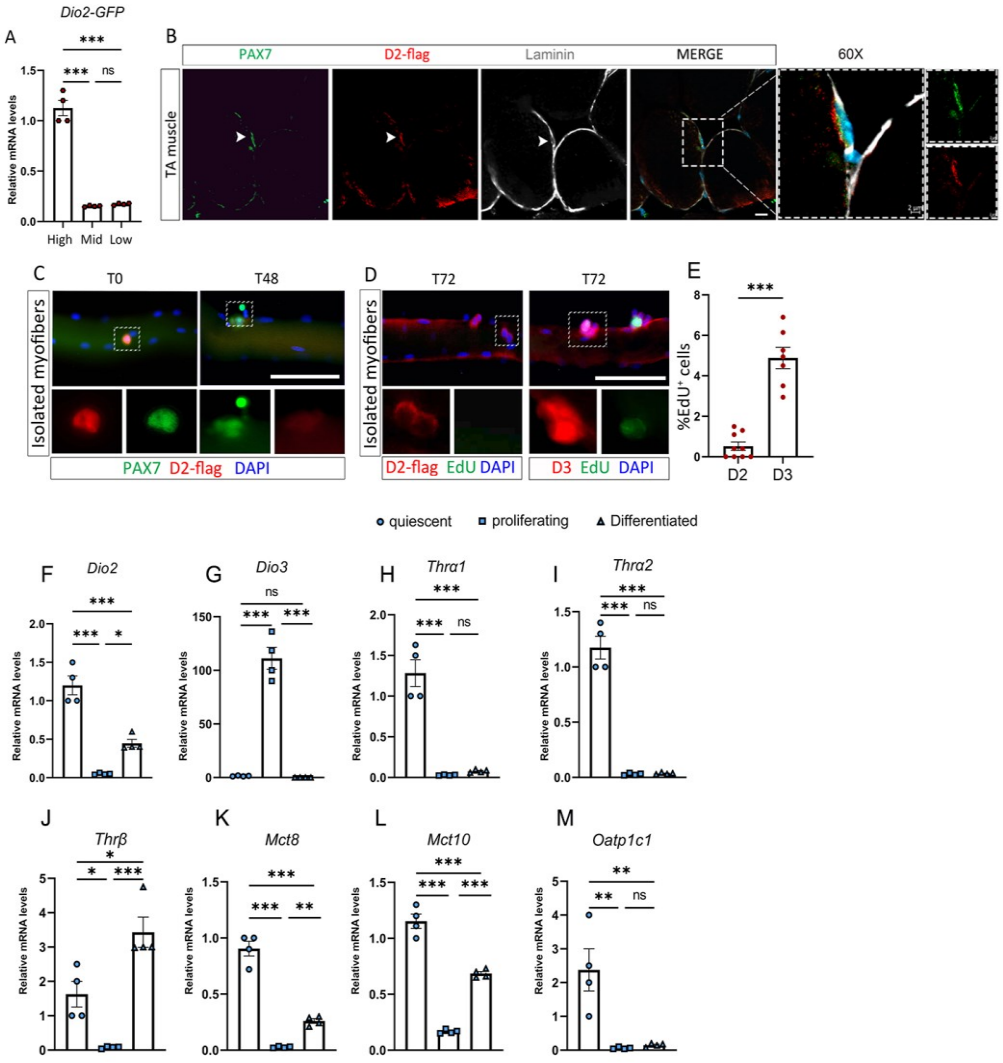

Figure 1. D2 is highly expressed in quiescent stem cells

(A) *Dio2*_mRNA levels in MuSCs high-mid-low freshly sorted from hindlimb muscle 3month old mice were evaluated by qRT-PCR (n=4 mice). (B) Representative immunofluorescence (IF) of Pax7, D2 and laminin co-localization. Confocal images of Pax7 (green), D2-FLAG (red), Laminin (white) and DAPI (blue) expression on cryo-sections of tibialis anterior (TA) muscle of D2-FLAG mice (Pax7-D2 co-localizations are indicated with arrowhead) (Scale bar, 10 µm), to the right original magnification: 63x (Scale bar, 2 µm). (C) Single myofibers with associated MuSCs were fixed either immediately after isolation (0 hr) or after 48 hr in culture and then immunostained for Pax7 (green) and D2-flag (red) (Scale bar, 50 µm). (D) Representative IF staining both for D3 that D2 *versus* EdU images in cultured fibers at 72 hours (Scale bar, 50 µm) (n=3 mice in three individual experiments). (E) Quantification of percentage EdU positive cells of D. (F)

Expression thyroid hormone profile for *Dio2*, (G) *Dio3* genes, (H) Thyroid receptors-α1 (*Thr-α1*), (I) Thyroid receptors-α2 (*Thr-α2*), (J) Thyroid receptors-β (*Thr-β*). (K) Thyroid trasporters *Mct8*, (L) *Mct10* (M) *Oatp1c1* in quiescence, proliferating and differentiated conditions were measured by qRT-PCR (n= 4).

4.2 Effects of TH treatment in MuSCs

Given the expression of D2 in quiescent muscle stem cells, we asked whether TH-treatment plays a role in stem cells *in vitro*. Freshly isolated FACS sorted $Pax7^+$ stem cells cultured with 20% FBS plus TH (3 nM T3 and 3 nM T4) for 8 days showed a reduced proliferation and S-phase measured by Pax7/EdU staining (Figures 2A-D "a" *versus "*b"). Interestingly, cells pre-exposed to TH for 4 days, promptly re-entered cell cycle upon removal of exogenous TH (Figure 2A, 2C-D, "c" *versus "*b"). Notably, the percent of $Pax7^+/EdU^+$ cells decreased and the percent of $Pax7^+/EdU^-$ cells increased in cells treated with TH only during the last four days (Figures 2A, 2C and 2D, "a" *versus* "d"). In summary, TH treatment delayed proliferation of stem cells while holding them in a reversible G_0 state.

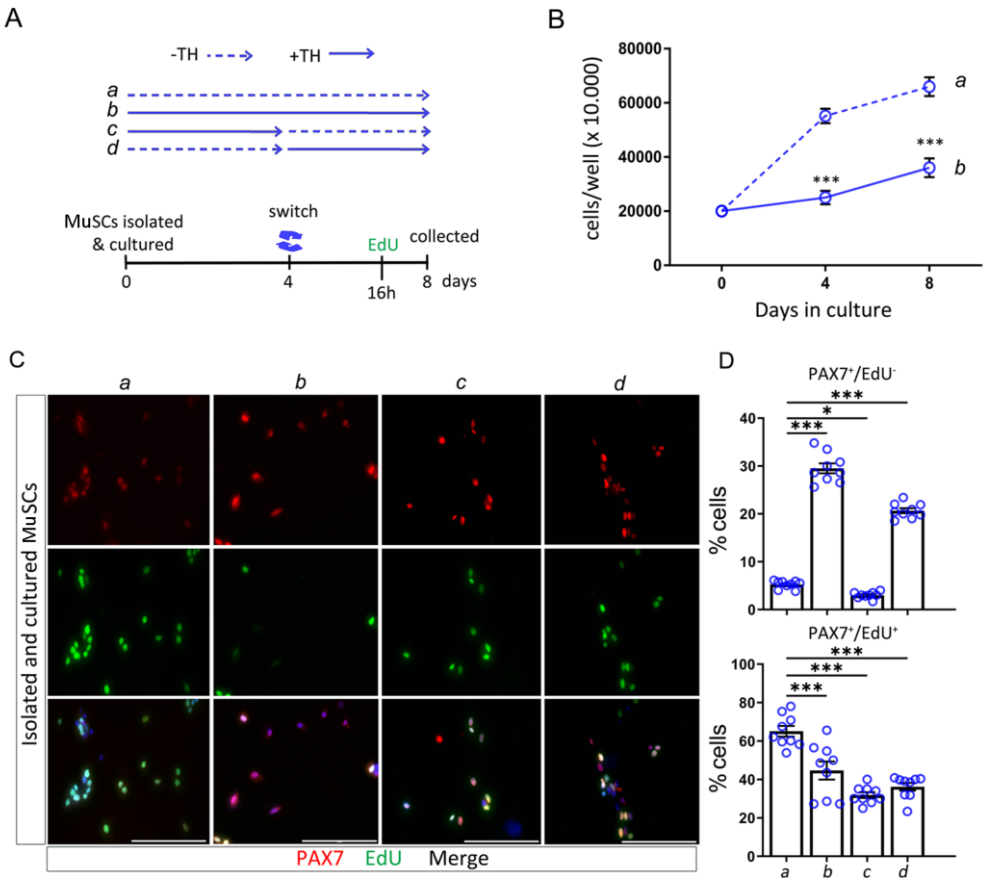

Figure 2. Thyroid hormone regulates exit of stem cells from the cellular cycle *(*A) Diagram of the switch experiment. FACS-sorted satellite cells were cultured for 8 days under the indicated conditions, and then pulsed with EdU for 16 h in culture. (B) Growth curve of MuSCs cultured in the absence or in the presence of TH. (C) Representative IF staining of Pax7 (red) and EdU (green) (Scale bar, 100µm). (D) Quantification of percentage of positive cells (Pax^{+}/Edu^{-} and Pax^{+}/Edu^{+}) of C. Results represent the average of 3 independent experiments.

4.3 Effects of D2-blocking in MuSCs

To assess the effects of D2 on stem cells, we blocked D2 action in cultured myofibers by treating them with rT3 (a specific D2 inhibitor) for 72 hours. Upon D2-blocking, we observed a reduced percentage of quiescent ($Pax7^{+}/MyoD^{-}$) cells and an increased percentage of activated ($Pax7^{+}/MyoD^{+}$) versus controls (Figure 3A). To assess in greater detail the role of D2 in MuSCs, we genetically ablated D2 in MuSCs by generating $Pax7^{CreERT2/+};D2^{fl/fl}$ mice (hereafter called cD2KO) in which TAM treatment induces D2 depletion specifically in MuSCs.

Consistent with rT3 treatment, genetic depletion *in vivo* of D2 in cD2KO by TAM treatment before culturing myofibers resulted in a lower percentage of $Pax7^{+}/MyoD^{-}$ cells, and a higher percentage of $Pax7^{+}/MyoD^{+}$ cells at various time points (Figure 1F). Double staining for Pax7/EdU on single myofibers revealed that the absence of D2 promoted the proliferation of MuSCs (Figure S3A). Accordingly, in myofibers treated with cytosine β-D-arabinofuranoside (ARA, a chemotherapeutic drug that kills cycling cells and spares resting cells), we detected fewer AraC-resistant $Pax7^{+}$ cells in the absence of D2 *versus* wt (Figure S3B), which suggests that D2-depleted MuSCs are more prone to exit quiescence and proliferate. These results indicate that, upon triggering of cell activation by the isolation procedure, blocking D2 in muscle stem cells boosts their proliferation.

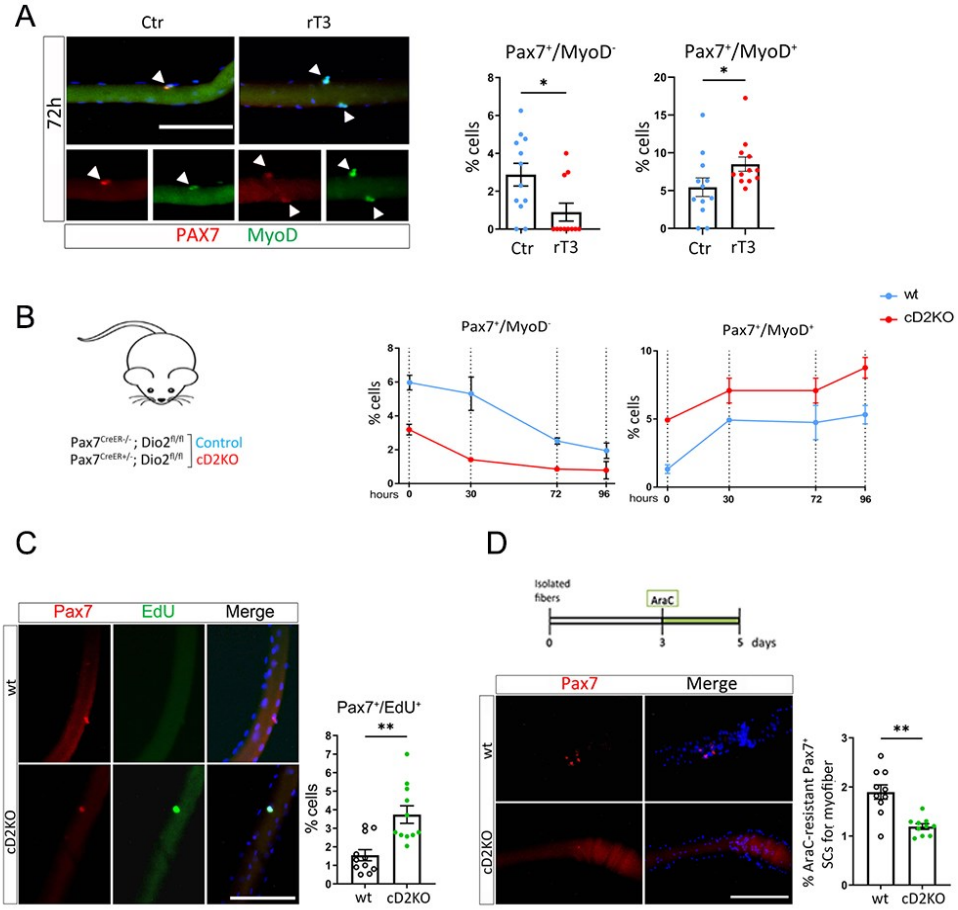

Figure 3. D2-depletion activates the MuSCs

(A) Representative IF staining of Pax7 (red) and MyoD (green) on isolated myofibers of D2 -3xflag mice +/-rT3 treated at 72 hours. (Scale bar, 100 µm), quantification of percentage positive cells (to the right) (ctr=4; rT3=4 mice in three individual experiment). (B) Quantification of percentage cells $Pax7^{+}/MyoD^{-}$, $Pax7^{+}/MyoD^{+}$ on isolated myofibers after tamoxifen induction of wt ($D2^{fl/fl}$ $Pax7^{creER\ -/-}$) and cD2KO mice ($D2^{fl/fl}$ $Pax7^{creER\ +/-}$) at different time (wt=5; cD2KO=4 mice in three individual experiment). (C) Representative IF staining EdU and Pax7 expression on myofibers isolated from 7 weeks old cD2KO and wt mice treated *in vivo* with TAM 4 days before sacrifice. Fibers were collected upon 36 hours in culture and pulsed with EdU 16 h before harvesting (wt=3; cD2KO=3 in three individual experiments) (Scale bar, 100µm), quantification of percentage positive cells (to the right). (D) Diagram of the experimental design and representative IF staining of Pax7 positive cells on cultured fiber treated with AraC for 48 hours (bottom) (Scale bar, 100µm); Percentage of AraC resistant $Pax7^{+}$ satellite cells (to the right) wt=5; cD2KO=5 in two individual experiments).

4.4 D2 deletion enhances stem cell proliferation during muscle regeneration

To determine the consequences of D2 depletion in MuSCs upon injury, we analysed TA muscles from cD2KO mice collected 21 days after Cardiotoxin (CTX) injection (Figure 2A). D2-depletion resulted in a greater number of centrally nucleated fibers *versus* control, associated with a smaller fibre diameter (Figures 2B-C). Accordingly, the number of $Pax7^{+}/MyoD^{+}$ cells, and the equivalent $Pax7^{+}/BrdU^{+}$ cells increased while the number of $Pax7^{+}/MyoD^{-}$ and the $Pax7^{-}/MyoD^{+}$ cell decreased (Figure 2D). This suggested that the absence of D2 increases the proliferative capacity of stem cells while the completion of myogenic program is delayed. This is in agreement with the delayed muscle differentiation we previously observed in global D2 knock-out mice (18). Interestingly, 60 days after CTX injury, fibre diameter was larger in cD2KO mice *versus* control, which suggests that complete maturation can be achieved with in the absence of D2 with prolonged time (Figure 2E).

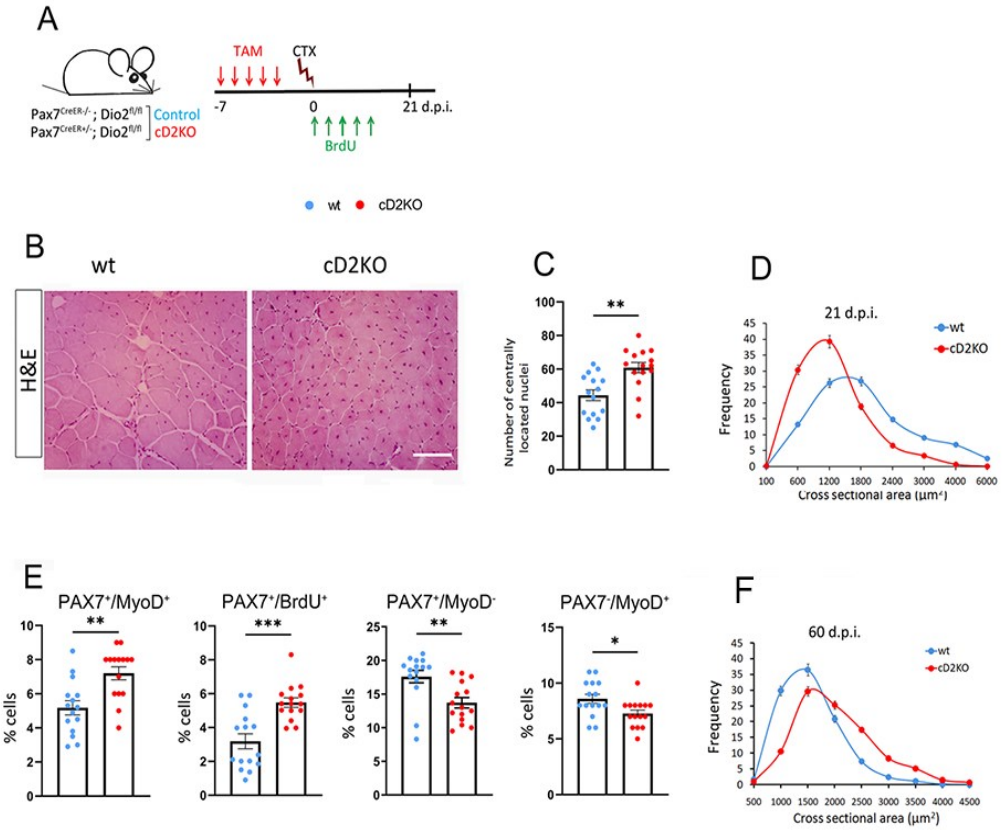

Figure 4. D2-depletion in quiescent MuSCs alters the regeneration
(A)Schematic diagram of the experimental design. (B) H&E staining of the TA sections from wt and cD2KO mice after TAM induction (Scale bar, 100 µm). (C) Percentage of centrally located nuclei evaluated of B. (D) Quantification of the cross-sectional area of TA sections of B. (E) Quantification of percentage positive cells by double staining Pax7/MyoD and Pax7/BrdU (wt n=5; cD2KO n=5 in three individual experiment). (F) Quantification of the cross-sectional area analysis of TA sections from cD2KO and wt (Pax7 $^{creER+/}$; R26^{mTmG}) adult mice 60 days after CTX-injection.

4.5 D2 is involved to restore the reserve of quiescent MuSCs in vitro

When proliferating MuSCs are induced to differentiate by serum deprivation of them elude terminal differentiation and become "reserve cells" (Pax7^{+}/MyoD^{-}) (31-33). The reduction in number of quiescent cells upon D2-depletion (Pax7^{+}/MyoD^{-} Fig 4E) prompted us to investigate whether D2 plays a role in the capacity of stem cells to constitute the "reserve population". In other words, we analysed whether activated MuSCs can re-enter quiescence in the absence of

D2. Upon induced differentiation (Figure 5A), we observed a reduced capacity to generate "reserve cells" ($Pax7^{+}/MyoD^{-}$) in the absence of D2 (Figure 5B). Accordingly, when we exposed MuSCs to serum deprivation and rT3, the number of $Pax7^{+}/MyoD^{-}$ reserve cells was lower than that of control (Figure 5B-C), which supports the concept that D2 is required to re-enter quiescence. Of note, D2-depletion was associated with increased number of activated cells ($Pax7^{+}/MyoD^{+}$) (Figure 5B-C) and a reduced myogenic differentiation (Desmin and MyHC2) (Figure 5D) which is in agreement with the role in promoting terminal differentiation subsequently played by a second surge in D2 during the differentiation program (18).

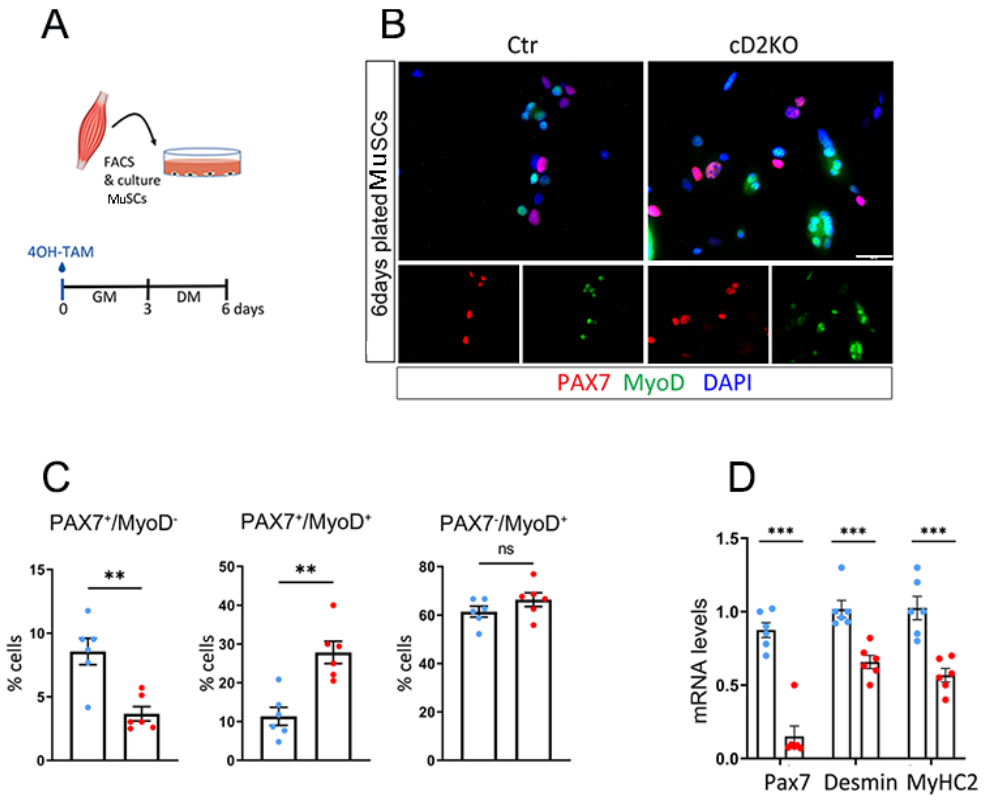

Figure 5. D2-depletion in quiescent stem cells alters the self-renewal
(A) Schematic design of "*reserve experiment*". (B) Representative immunostaining of Pax7 (red) and MyoD (green) on MuSCs 6 days after plating in the presence or absence of 1µM 4OH-Tam isolated from D2 $^{fl/fl}$ Pax7 $^{creER\ +/-}$ (Scale bar, 200 µm). (C) Quantification of percentage positive cells by double staining Pax7/MyoD. (D)

Pax7, Desmin and MyHC2 mRNA levels were evaluated by qRT-PCR (Ctr=3; cD2KO=3 in two individual experiment).

4.6 D2 is required for self-renewal of quiescent MuSCS in vivo.

To evaluate whether the observed reduced number of quiescent ($Pax7^{+}/MyoD^{-}$) cells upon injury (Figure 4E) reflects the inability to restore the stem cell reservoir in the absence of D2, we investigated whether D2-depleted stem cells could normally re-constitute the stem cell pool *in vivo*. To this aim, we analysed muscle repair after five consecutive CTX injuries at 30 days after the last CTX (Figure 6A). In this setting, the number of quiescent satellite cells ($Pax7^{+}/MyoD^{-}$) was lower in cD2KO mice (Figure 6B). Furthermore, in D2-depleted muscles after multiple injuries, areas of non-muscle tissue were larger than control (Figures 6C and D), while the diameter of the newly formed muscle fibers was reduced (Figure 6E). Accordingly, we found increased intramuscular fibrosis, which confirms MuSCs failure in cD2KO upon consecutive damages (Figures 6F and G). Overall, these data indicate a self-renewal deficiency of D2-depleted stem cells that leads to a gradual depletion of resident stem cells and consequent increased fibrosis after muscle injuries. Accordingly, by using a different mouse model ($Pax7^{CreER+/-}$; $^{/+}$; $R26^{mT/mG}$; $D2^{fl/fl}$ *versus* $Pax7^{CreER+/-}$; $R26^{mT/mG}$; $D2^{+/+}$), in which green epifluorescence labels newly generated D2-depleted fibers, we observed that newly generated D2-depleted green fibres were fewer but larger in absence of D2 *versus* control after three consecutive CTX injuries (Figures 6H-J). Moreover, *Pax7* and *MyHC2* mRNA levels were lower in triple injured cD2KO muscle than in control (Figure 6K). These results suggest that after multiple injuries MuSCs fail to repopulate the stem cell reservoir in cD2KO mice.

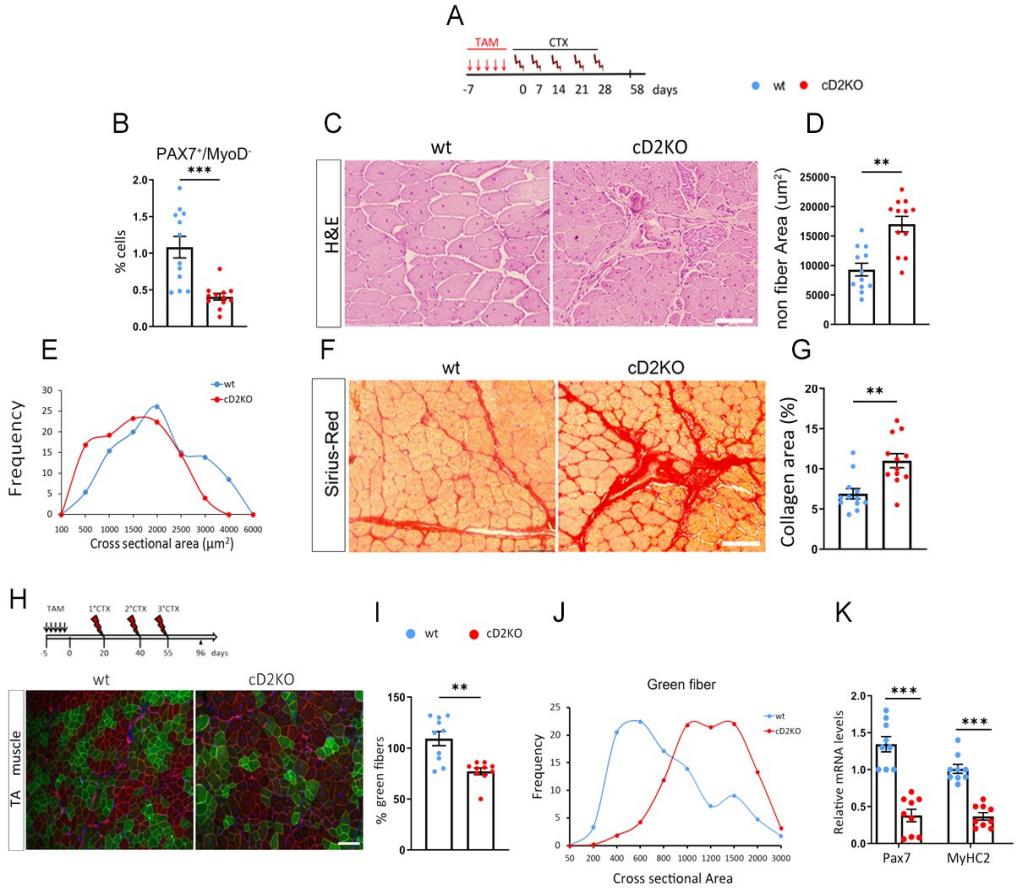

Figure 6. Absence of D2 negatively affects satellite cell pool upon multiple rounds of regeneration

(A) Schematic experiment of CTX-multiple. (B) Quantification of percentage of positive cells by double staining Pax7/MyoD. (C) H&E from cD2KO and wt (Scale bar, 75 µm). **(D)** Quantification of the percentage of non-myofiber tissue over the total section area of C. (E) Quantification of the cross-sectional area of C. (F) Representative Sirius-red staining of TA sections from cD2KO and wt mice (Scale bar, 75 µm). (G) Quantification of the percentage of collagen area. (A-G) wt n=4; cD2KO n=4 mice in three independent experiments. (H) Diagram of the experimental design of triple CTX from $Pax7^{CreER\ +/-}$ $R26^{mT/mG}$; $D2^{fl/fl}$ or $Pax7^{CreER-/-}$ $R26^{mT/mG}$; $D2^{+/+}$), mice; Representative green epifluorescence (labeling newly generated fibers) on TA muscle, bottom. (I) Percentage of green fibers. (J) Quantification of the cross sectional area of green fibers of figure A. (K) Pax7 and MyHC2 mRNA levels measured by qRT-PCR (wt n=5; cD2KO n=5 mice in two individual experiments).

4.7 D2-derived TH sustains the Notch pathway

To shed light on the molecular mechanisms triggered by D2 depletion in quiescent stem cells, we purified MuSCs by magnetic separation from cD2KO *versus* ctr mice in resting muscle and analysed the cell transcriptome by RNA-sequencing analysis immediately thereafter. About thirteen hundred genes were significantly altered in cD2KO MuSCs *versus* controls, of which approximately half were downregulated and half were upregulated (Figure 7A). Functional analysis identified multiple pathways affected by D2-depletion (Figures 7B-C); among the pathways downregulated by D2-depletion, the Notch signaling pathway stand out as a potential regulator of stemness (Figure 7B). We validated this finding in FACS isolated Pax-nGFP^{+} cells, and found that relevant Notch targets (*HeyL, Hes2 and Rbpj*) and Notch receptors (*Notch1, Notch2, Notch3 and Notch4*) were downregulated at the mRNA level in cD2KO MuSCs (Figure 7D). Importantly, Western blot revealed lower levels of the active Notch Intracellular protein (NICD) in D2-depleted cells (Figure 7E). We next evaluated whether TH nuclear receptor directly binds Notch receptor loci. In silico analysis revealed the presence of multiple putative TH-responsive-elements (TRE) in the locus of two Notch receptors, i.e. Notch2 and Notch3 (Figure 7F). Chromatin immunoprecipitation (ChIP) assay confirmed the binding of TH receptor (TR) to one site of Notch2 and one of Notch3 (3 and 38-fold enrichment respectively in the presence of TR antibody; Figure 7G). In conclusion, these experiments suggest that, in MuSCs D2 is an upstream regulator of Notch that acts via a direct TRα-mediated transcriptional regulation of Notch receptor 2 and 3. To assess whether active Notch could functionally rescue D2 depletion *in vivo*, we generated Pax7$^{CreER+/-}$; D2$^{fl/fl}$; R26$^{stop\text{-}NICD\text{-}nGFP}$(thereafter referred to as cD2KO-N1ICD) mice in which D2 was excised in MuSCs with simultaneous Notch activation. We characterized the MuSCs population in regenerating TA muscles at 21 (Figure 7H) days after CTX of cD2KO/N1ICD and cD2KO mice. Immunofluorescence staining showed a reduction of the percentage of Pax7^{+}/EdU^{+} cells (as well as Pax7^{+}/MyoD^{+} cells) and a corresponding increase in Pax7^{+}/EdU^{-} cells in cD2KO/N1ICD mice *versus* control (Figures 7H-I), which indicated that the effects of D2 depletion was substantially rescued by Notch overexpression. These data show that D2 is required to sustain Notch signaling in quiescent stem cells, and that forced Notch activity can rescue some of the effects of D2-depletion.

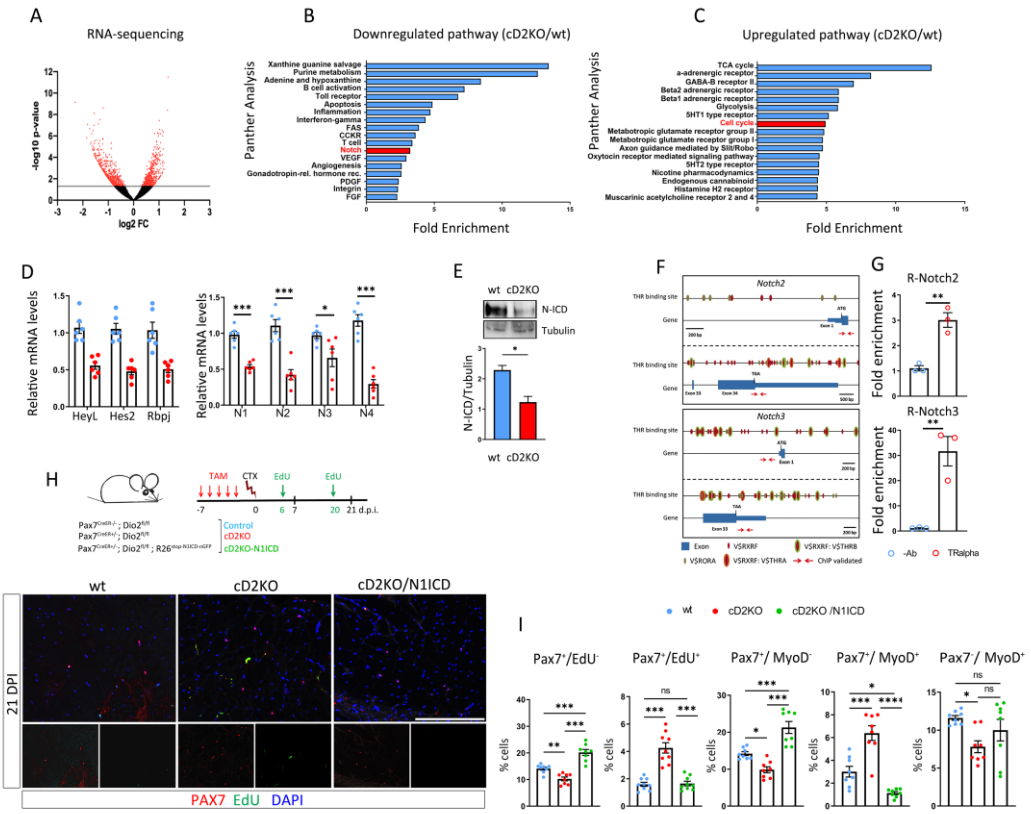

Figure 7. D2 is required for the maintenance of quiescence by sustaining the Notch pathway

(A) Volcano plot showing differences in the mRNA expression of cD2KO qMu SCs and wild type controls. The negative log10 p-value (y-axis) and log2 fold change (FC; x-axis) are plotted for transcripts detected by RNA-seq analysis (gray line indicate p-value<0.05; n=3 biological replicates). (B) The most significant downregulated Panther (Protein Analysis Through Evolutionary Relationships) pathways. (C) The most significant up-regulated Panther pathways. (D) mRNA levels of Notch targets (Hey-L, Hes2 and Rbpj) and Notch receptors (1-2-3-4) in wt and cD2KO qMuSCs isolated by FACS, were measured by qRT-PCR. (wt n=3; cD2KO n=3 mice in two independent experiments). (E) Protein levels of NICD measured by western blot in wt and cD2KO qMuSCs. Tubulin serves as a loading control. The graph to the right shows the quantification of NICD/tubulin. (F) 3' and 5' flanking regions of the mouse Notch2 and Notch3 genes. (G) C2C12 cells were processed for ChIP using THR-alpha antibody and the isotype control antibodies, followed by qRT-PCR for Notch2 and Notch3 receptors. The data are normalized for background levels and input chromatin for each sample. (H) Diagram of rescue exdperiment *in vivo*. (I) Representative IF of Pax7/EdU in TA sections from wt, cD2KO and cD2KO/N1ICD mice harvested 21 days after CTX-injection (Scale bar, 200µm). Quantification of percentage positive cells for Pax7/Edu of H, and

Pax7/Myod (image not shown). (I) wt n=4; cD2KO n=4 cD2KO-N1ICD n=4 mice in two independent experiments.

4.8 D2 regulates the entry of quiescent MuSCs into a G_{Alert}- state in resting muscle

Quiescent MuSCs can cycle between two molecular states: a dormant (G_0) state and a primed but still non-dividing state (G_{Alert} state) induced in response to generalized tissue injury. The G_{Alert} phase is characterized by increased cell size, mitochondrial DNA, a rapid entry into cell cycle, and dependency on the mammalian target-of-rapamycin (mTORC1) (11). In MuSCs isolated from resting muscle, "Cell cycle" was among the upregulated pathways induced as a consequence of D2-depletion (Figure 7C). FACS counting of Edu^+/Pax7-$nGFP^+$ cells revealed that the number of D2-depleted cells exceeded than of control, and moreover that it reached a percentage level comparable to the wild type "Alerted cells" (Figures 8A-B). However, D2 depletion alone was unable to fully activate cell proliferation as induced by injury (Figure 8A-B). To assess whether D2-depletion in MuSCs is able by itself to "alert" cells, we measured known markers of the G_{Alert} state in resting muscle. This experiment showed that D2-depletion activates mTORC1 as witnessed by increased levels of phospho-mTOR (Figure 8C), its target phospho-S6-ribosomal protein (Figure 8D) and phospho-S6K (Figure 8E). Activation of the mTOR pathway could depend on the reduction of AMPK activity, which in turn regulates mTOR. Interestingly p-AMPK was potently downregulated by D2-depletion (Figure 8F), which suggests a mechanism by which D2-depletion increases mTORC1 by attenuating AMPK activity. Moreover, we found that D2-depleted MuSCs have increased mitochondrial DNA content (Figure 8G) and are larger than wt MuSCs as measured by FACS (Figure 8H). Thus, these findings indicated that D2-depletion can induce an "Alert state" in MuSCs.

In parallel, we also evaluated whether a change in D2 levels also occurs in "alerted" MuSCs. Interestingly, D2 was drastically lower in G_{Alert} cells than in quiescent G_0 cells (Figure 8I), which is in consonant with a role that D2plays in the "alerting" process. Lastly, we compared in silico the genes differentially expressed in cD2KO *versus* control MuSCs (Figure 8A) with those induced in the G_{Alert} state deposited in the GSE55490 database (11). Interestingly, of the 678 down-regulated genes in cD2KO, 52 overlap with the down-regulated genes in G_{Alert} state ($p < 2.418^{e-16}$); while of the 611 up-regulated genes in cD2KO, 26 overlap with the up-regulated genes in G_{Alert} state ($p < 0.041$) (Figures 8J and K). Overall, these data indicate D2 depletion causes a condition whose transcriptionally signature significantly overlap with the G_{Alert} state and support the finding that D2-depletion – is sufficient alone to cause- an "Alerted state" in muscle stem cells.

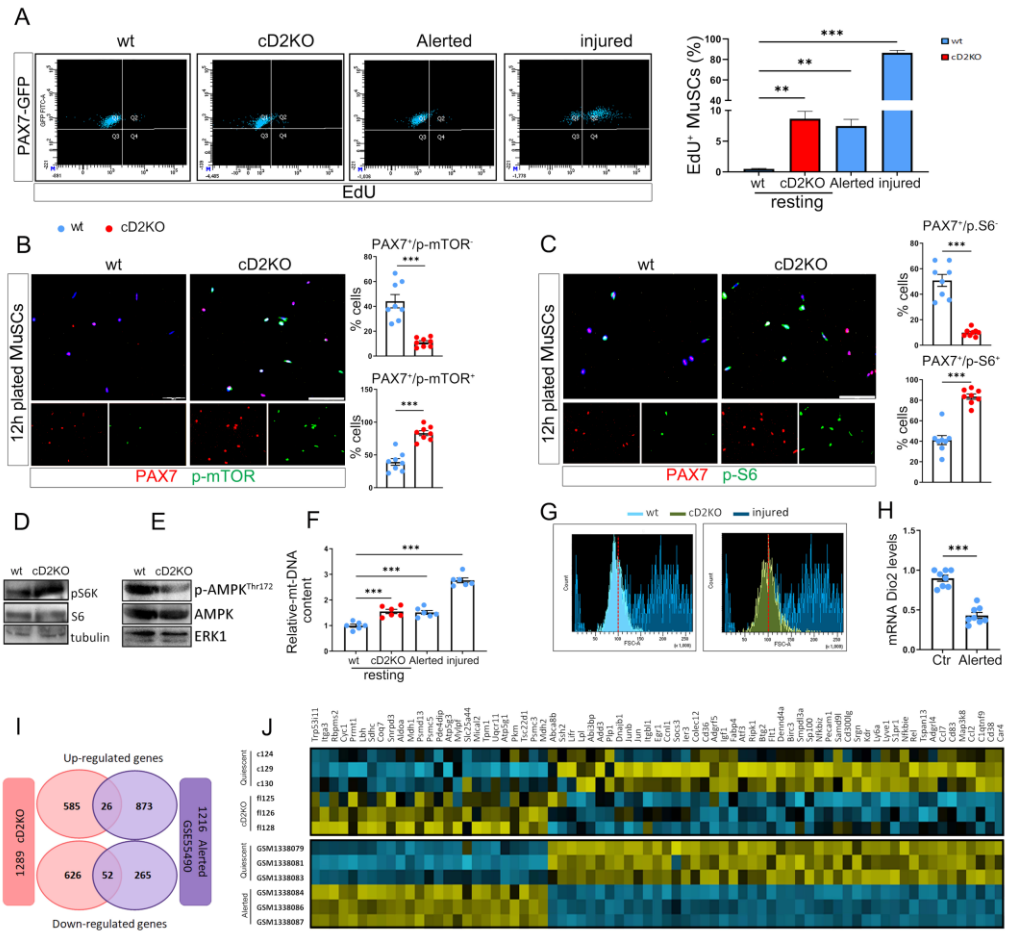

Figure 8. In resting muscle, D2 depletion turns qMuSCs in an "alerted state"
(A) EdU incorporation of qMuSCs *in vivo* by FACS. Percentage of MuSCs that incorporated EdU (right). Results are average of 3 independent experiments. (B) Representative IF of PAX7 (red) and p-mTOR (green) on MuSCs freshly isolated from wt and cD2KO mice (Scale bar, 200μm); quantification of percentage positive cells (right). (C) Representative IF of PAX7 (red) and p-S6 ribosomal protein (green) on MuSCs freshly isolated from wt and cD2KO mice (scale bar, 200μm); quantification of percentage positive cells (right). In (B) and (C) used wt=4; cD2KO=4 mice in two independent experiments. (D) Representative immunoblot of protein pS6K and total S6K, from cD2KO and wt MuSCs were measured by western blot. (E) Representative immunoblot of phospho-AMPK and total AMPK by western blot. (F) Mitochondrial DNA from MuSCs wt, cD2KO (resting), alerted and injured (3 mice each group in two independent experiments). (G) Representative FACS histogram of forward scatter (FSC) signal of MuSCs from wt (light blue), cD2KO (green) and injured (blue) mice. (H) D2 mRNA expression from muscles of ctr (not injured) and contralateral (alerted) MuSCs wt mice, isolated 2 days after CTX-injury by FACS. (Ctr=4; Alerted=4 muscles in two independent experiments). (I) Vienn comparison analysis between cD2KO RNA-seq and G_{Alert} state array described by Rodgers et al., 2014, common genes down-regulated ($p < 2.418e-16$) and common genes up-regulated ($p < 0.041$). (J) Heatmap comparison of common genes up/down- regulated from cD2KO RNA-seq *versus* Ctr and G_{Alert} state array *versus* Ctr described by Rodgers et al., 2014.

4.9 Characterization of the phenotype of the mdx-D2KO mice

Premature exhaustion of MuSCs is a major determinant of the dystrophic process (34, 35). We asked whether D2-depletion could affect the dystrophic phenotype of *mdx* mice. To this aim, we generated the *mdx*/global-D2 knock-out (*mdx*-D2KO) mice and characterized the muscle phenotype by morphological and molecular analyses. We measured Pax7 and neo-MHC mRNA levels in a period from 4 to 50 weeks postnatally, and found that both markers were higher in *mdx*-D2KO mice *versus* control (Figure 9A). Increased number of $Pax7^+$ cells were also detected in TA muscle in *mdx*-D2KO mice vs control *mdx* (at 4 weeks post-natal, which is the peak of dystrophy) (Figure 9B). At 4 weeks, while fiber size in *mdx*-D2KO mice was smaller, the number of fibers was increased (Figures 9C-E). In addition, the levels of myogenin and MyoD were higher whereas the levels of Creatine Kinase (CK) lower in *mdx*-D2KO mice versus control (Figure 9F). Thus, global D2-depletion in *mdx* context results in a delayed dystrophic

phenotype, a significantly increased number of muscle stem cells associated with and more temporally sustained regenerative potential.

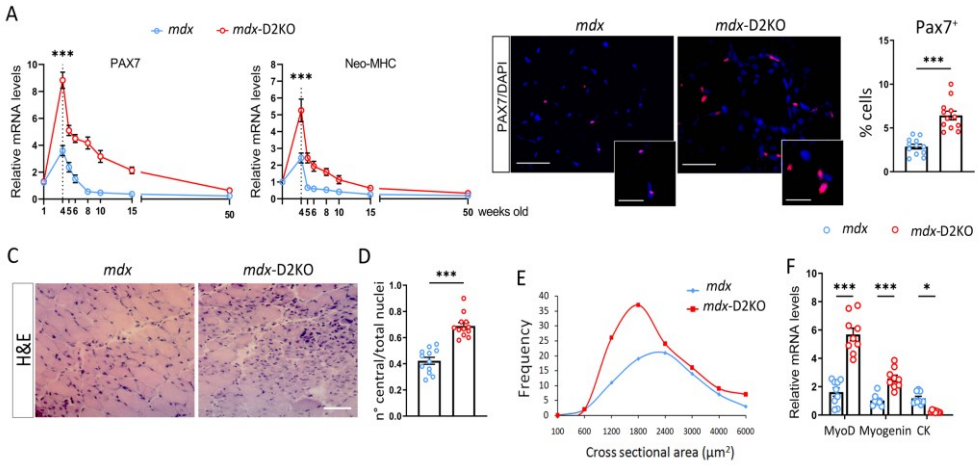

Figure 9. Phenotype's characterization of Mdx-D2KO mice

(A) Pax7 and neo-MHC mRNA levels from wt and total-D2KO *mdx*-mice were measured by qRT-PCR at different time points. (B) Representative IF and its quantification (right) of Pax7/DAPI of TA sections from wt and total-D2KO of *mdx*-mice 4 old weeks (Scale bar, 100 µm and 50 µm). (C) Representative H&E-stained TA sections from wt and total-D2KO *mdx*-mice 4 old weeks (scale bar, 100 µm). (D) Percentage of centrally located nuclei of C. (E) Quantification of the cross-sectional area distribution of C. (F) Myogenin, MyoD and Creatin Kinase mRNA levels were measured by qRT-PCR. (B-F) *mdx* *n*= 4; *mdx*-D2KO n=4, of three individual experiments.

4.10 Transplantation assays to evaluate cell engrafting potential in vivo after D2-depletion in mdx background

Based on the data obtained with the *mdx*-D2KO mice, we tested the functional capability of D2-depleted MuSCs to engraft *in vivo* by conducting a transplantation assay. We isolated MuSCs from donor $Pax7^{CreER+/-}$; $R26^{mT/mG}$; $D2^{fl/fl}$ [1] *versus* $Pax7^{CreER+/-}$; $R26^{mT/mG}$; $D2^{+/+}$) mice and injected these into the TA of *mdx* mice (Figure 10A). Engraftment of donor-derived myofibers in *mdx* recipients was analysed by direct epifluorescence for green fluorescent protein

on TA muscle harvested 21 and 40 days after transplantation (Figure 10B). The number of GFP-positive D2-depleted fibres was increased at both 21 and 40 days after transplantation (Figure 10C) which is in agreement with the enhanced proliferation rate of D2-depleted cells. Cross sectional area (CSA) analysis showed that- D2-depleted fibres were smaller at 21 days and larger at 40 days *versus* control, which indicates that D2-deficiency could be compensated at a later time (Figure 10D), which is in agreement with D2-depletion *in vivo* (Figures 4D and 4F). Overall, there results indicate that D2-depleted MuSCs successfully engraft, have an increased proliferative capacity and a time-dependent delay in maturation that is compensated at later time points.

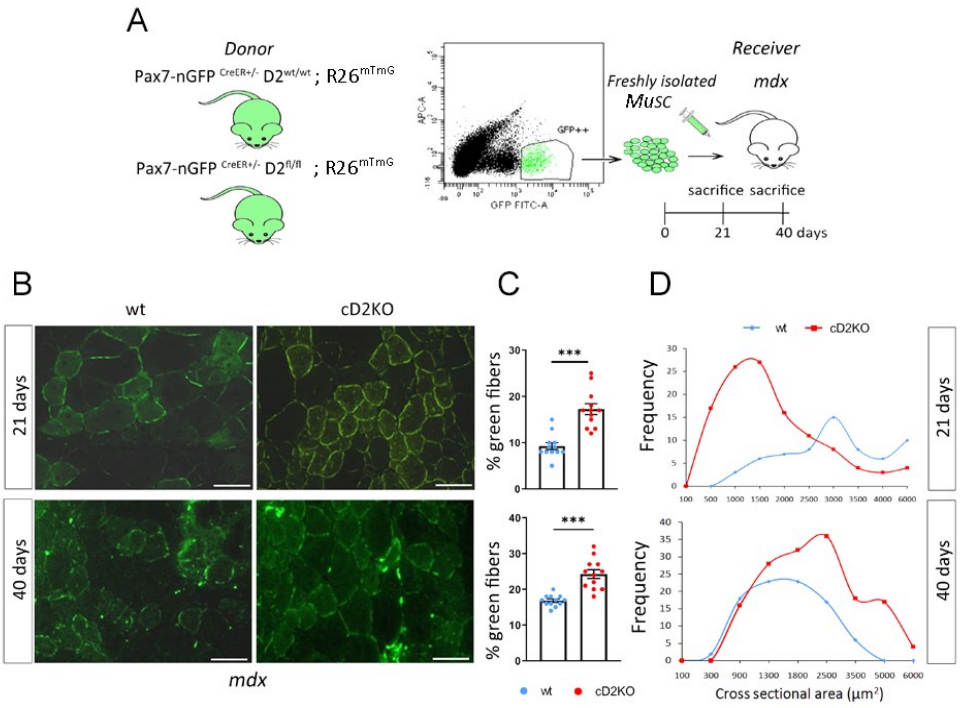

Figure 10. Xenograft studies into MDX mice

(A) Experimental design of FACS-isolated MuSCs from wt (Pax7-$^{creER+/-}$ D2$^{+/+}$; R26^{mTmG}) and cD2KO (Pax7-$^{creER+/-}$ D2$^{fl/fl}$-; R26^{mTmG}) mice and transplanted in the left and right TA muscles respectively in *mdx*-mice. (B) Representative green epifluorescence of wt and cD2KO fibers into mdx mice after 21 and 40 days post xenograft. (Scale bar,100 µm). (C) Percentage of GFP fibers (green) 21days (top) and 40 days (bottom) following transplantation. (D) Quantification of the cross-

sectional area after 21 and 40 days from engraft. (A-D) wt n= 4; cD2KO n=4 receiver mdx mice of three independent experiments.

4.11 D2-depletion affects stem cell homeostasis in skin

To assess whether D2 expression in stem cells is limited to the muscle or is a common feature shared by other tissues, we analyzed the localization of D2 in skin. Interestingly, D2 expression co-localized with the hair follicle stem-cell marker CD34, which specifically marks the bulge of the hair follicle, which is where quiescent stem cells are localized (Figure 11A). In addition, we found that D2 expression was dynamically regulated during the hair follicle cycle. In fact, D2 was clearly detectable in the telogen phase, the resting phase of the hair follicle cycle, and never coincided with EdU labelling (Figure 11B). To investigate the role of D2 in the hair follicle stem cells we generated a skin conditional D2KO (scD2KO) mouse model ($K14^{CreER+/-}$; $D2^{fl/fl}$). Interestingly, the percentage of $CD34^{+}$/alpha 6 $integrin^{+}$ cells (hair follicle stem cell markers), significantly increased 6 days upon D2-depletion (Figure 11C). These results indicate that, similar to what we observed in muscle, blocking D2 in hair follicle stem cells, promotes their proliferation. Next, we analysed the effects of specific D2-depletion in the hair follicle compartment of mice subjected to one (T1) or three (T3) consecutive rounds of hair depilation. We observed that the number of $Sox9^{+}$/ EdU^{+} cells in the hair follicle bulges increased upon D2-depletion after a single round of depilation (T1), while three rounds of depilation caused a net decrease in the EdU^{+} and $Sox9^{+}$ cells (Figure 11D). Accordingly, Sox9 and CD34 mRNA were initially increased at T1, and reduced at T3 (Figures 11E), thus suggesting that while D2 depletion initially increased the activation of stem cells, it caused cell exhaustion following subsequent rounds of amplification. To characterize the effects of D2-depletion *in vivo* during tissue regeneration, we performed a wound healing assay. The time course of regenerating epidermis showed that the closure of the wound was significantly faster in D2-depleted epidermis than in control skin (Figure 11F). Overall, these data indicate that D2 plays a key role in preserving hair follicle stem cells from uncontrolled activation.

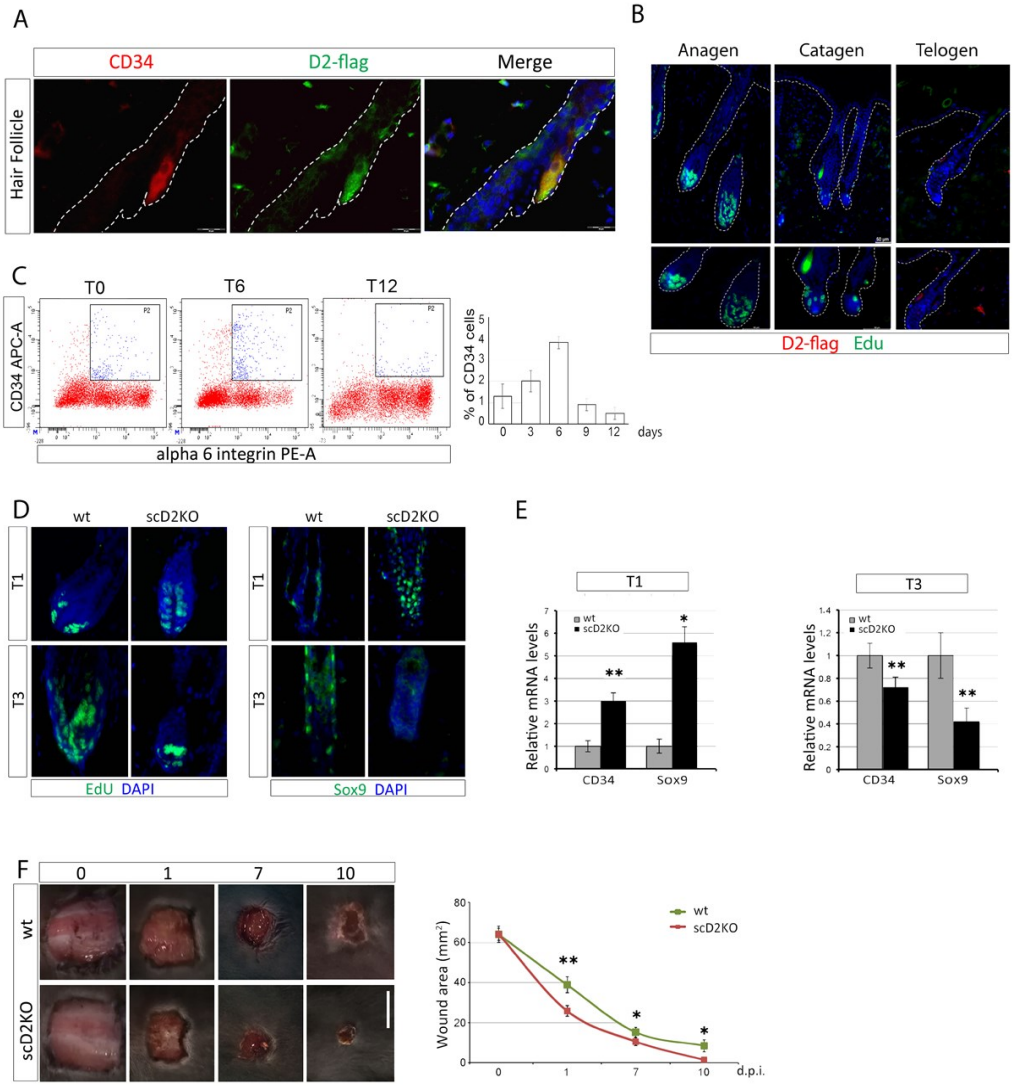

Figure 11. Functional characterization of D2 expression in mouse skin

(A) Representative IF staining of CD34 (red) and D2-3xFLAG (green) expression in the hair follicle of the epidermis (scale bar). (B) Representative image of EdU positive cells (green) and D2 positive cells during the hair follicle cycle (scale bar). (C) The number of CD34-positive cells was evaluated by FACS analysis of α6-integrin $^{+}$ /CD34 $^{+}$ cells in the epidermis of K14$^{Cre+/-}$-D2$^{fl/fl}$ mice at 0 (T0), 6 days (T6) and 12 days (T12) after tamoxifen-induced D2 depletion. (D) EdU positive cells and Sox9 positive cells in the hair follicle after one (T1) and three (T3) consecutive shavings in K14$^{Cre\ +/-}$ D2$^{fl/fl}$ mice and K14-$^{Cre\ -/-}$ D2$^{fl/fl}$ mice (wt and scD2KO respectively). (E) CD34 and Sox9 mRNA expression were measured by qRT- PCR in the same experiment as in E. (F) Wound Healing experiment in scD2KO mice (and wt mice following tamoxifen-induced D2 depletion. Representative images of the wound area at 0, 1, 7 and 10 days following the wound

healing. Wound area was calculated by the Cell*F Olympus Imaging Software (Scale bar, 1 cm).

4.12 Drug-induced D2-inhibition as therapeutic tool to enhance expansion of activated precursor cells.

To therapeutically exploit the capacity of D2-depletion to alert stem cells and accelerate muscle tissue repair, we treated mice with oral rT3 (a specific D2-inhibitor) for 7 days (-5/+2 relative to CTX injury) (Figure 12A). Hematoxylin & Eosin (H&E) analysis 7 days post-CTX revealed more fibers in rT3 treated than in control mice (Figures 12B and C). In rT3 treated mice, $Pax7^{+}/EdU^{+}$cells were increased and fibers were smaller than control mice (Figure 12D). Importantly, 21 days after injury we observed larger fibers in rT3 treated mice than control, which is in agreement with the limited time frame (7 days) of D2 inhibition (Figures 12E and F). In a similar setting, we tested whether D2 inhibition positively affected wound regeneration in skin, and found that rT3-treated mice repair wounds more rapidly and efficiently than control mice (Figures 12G).

In summary, we demonstrated that drug-induced D2-blocking with rT3 facilitates regeneration, -likely alerting stem cells-, in different tissue contexts and could be therapeutically exploited *in vivo*.

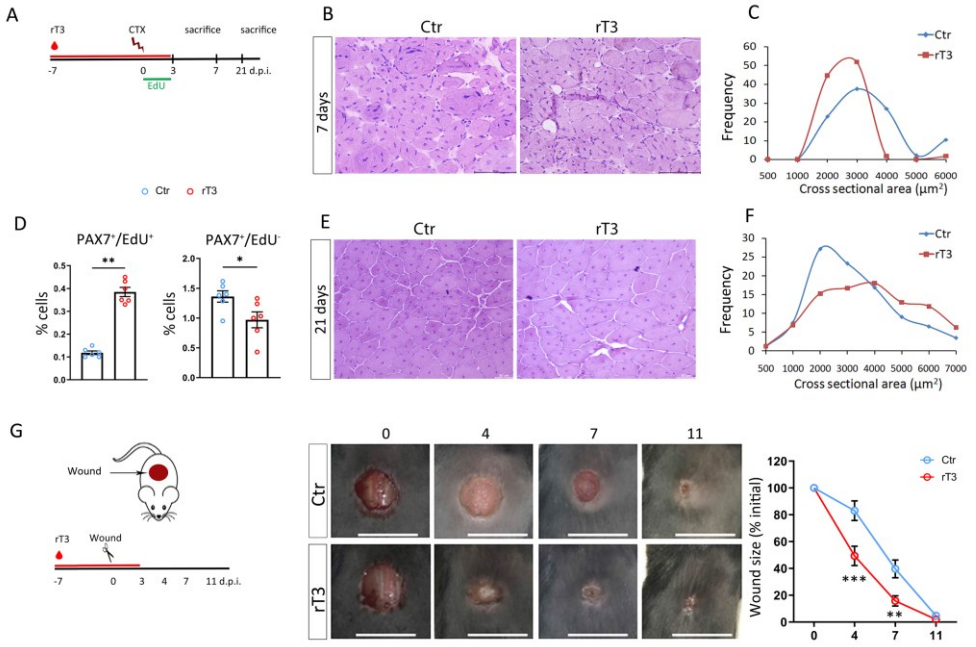

Figure 12. rT3 as novel therapeutic agent to to enhance expansion of activated precursor cells.

(A) Scheme of the experimental design. (B) Representative H&E from TA sections from rT3-treatment and ctr mice, sacrificed 7 days after CTX-injury (Scale bar, 50µm). (C) Quantification of the cross-sectional area of B. (D) Percentage of Pax7/EdU staining on TA sections from rT3-treatment and ctr (Ctr=3; rT3=3 mice in two individual experiments). (E) Representative H&E from rT3-treatment and Ctr mice, sacrificed 21 days after injury (Scale bar, 50µm). (F) Quantification of the cross-sectional area of E. (G) Scheme of the experimental design and representative images of skin wound healing in mice treated with rT3 versus control. To the right, quantification of wound closure is presented as the mean of the percent of initial wound size (n =4 each group in four independent experiments) (Scale bar, 1cm).

5. DISCUSSION

Cellular quiescence is a property of several adult vertebrate stem cells. How this condition is regulated and preserved is a central issue in stem cell biology which still remains poorly understood. Here we report that D2 is a key metabolic enzyme that acts as a master regulator of muscle stem cell quiescence. The D2 - mediated action represents a functional link between the circulating thyroid hormone concentrations and a cell-autonomous mechanism that enables to customize intracellular TH and preserve quiescence and stem cell function. The temporal expression pattern of D2 is peculiar. Indeed, the *Dio2* mRNA is elevated in quiescence, drastically reduced upon activation and back on at a later phase of myogenesis to allow full differentiation (Figure 1F). Our data indicate also that in activated stem cells D2 is re-expressed in a subset of cells and this is relevant for return to quiescence and to restore the normal stem cell reservoir under normal conditions (Figure 3A-D). In the absence of D2 activity, proliferating myoblasts fail to self-renew and this would eventually cause depletion of the stem cell pool (Figure 6A-K). The role of D2 in quiescence is unknown. We propose that the thyroid hormone producing D2 acts as a sensor/effector rheostat of the normal environment by increasing intracellular TH concentrations in stem cells to preserve the quiescence state. TH acts in several cell context as a pro-differentiating agent (18, 36) and the increased TH concentration in resting muscle stem cells is likely a mechanism to defend quiescence from undesired breaking signals present in the micro-environment. In this setting, D2-produced increased TH acts as a cell autonomous signals that sustain stem cell quiescence. Upon disruption of the niche, D2 is sharply downregulated in stem cells thereby causing these cells to exit quiescence. The signals regulating D2 expression in quiescent cells are presently unknown and the represent the aim of future studies. While it is well known, from clinical observation in patients with thyroid disfunction, that thyroid hormone influences tissue homeostasis and regeneration, the identification of the TH producing enzyme D2 specifically expressed in quiescent stem cell compartment both in muscle and skin add TH signaling as a key player in the mechanisms controlling quiescence, tissue homeostasis and regeneration.

D2 is, to our knowledge, the only TH related protein known to keep and preserve quiescence in solid organ stem cells. Our data indicate that D2 gene program affects stem cell niche in the skeletal muscle as well as in other tissues such as

the skin (Figure 11) and the brain (data not shown) which also specifically express D2 in the stem cell compartment. What are the molecular mechanisms by which D2 controls quiescence? Our RNA seq analysis from quiescent muscle stem cells isolated from cD2KO vs control revealed that the Notch signaling is down-regulated at multiple level upon D2 genetic depletion (Figure 7B). The Notch pathway has been found to be a key regulator of many types of adult stem cells, and its activity has been shown to be instrumental for the regulation of cell fates and proliferation in a variety of tissues. Quiescent muscle stem cells are characterized by elevated Notch activity that is required for their maintenance. By Chromatin immunoprecipitation, we could demonstrate that TH receptor alpha directly binds to the Notch1 and Notch3 gene locuses and promote their expression (Figure 7G). The functional association between Notch and D2 firstly derived from the expression profile in Pax7-nGFP subsorted cells wherein – in the GFP^{high} subpopulation- both D2 and Notch activity are highest (Dentice et al, 2014 (23) and Figure 1A). Using different combinations of genetically modified mice of D2 and Notch altered levels, we identify D2 located epistatically upstream of Notch in quiescent stem cells. Notch signaling is necessary and sufficient for preserving quiescence and could rescue the phenotype observed upon D2 depletion. In fact, imposed contemporary expression of active Notch substantially rescued the phenotype of D2-depletion *in vivo* (Figure 7A-K). However, we measured Notch rescue by the analysis of few markers (Figure 7A-K) and given the pleiotropic effects of TH it is likely that other genes/pathways are regulated by TH and influence satellite cell behaviour which are not compensated by Notch overexpression. Of note, the role of Notch signaling in actively promoting the self-renewal of muscle stem cells through direct regulation of Pax7 is also consistent with the reduced self-renewal observed in cD2KO cells, sustaining the idea of a large overlapping and upstream position of TH respect to the Notch signaling. In any case, our studies specifically identified Notch signaling as a principal mediator of TH in controlling the quiescent state, which illustrate a novel mechanism TH-dependent of satellite cell control of quiescence. Of note, our study not only delineates a D2-mediated molecular mechanism by which locally produced TH concentration is increased in quiescent stem cell, but also demonstrates the importance of such a TH- Notch- axis in regulating normal stem cell function. What are the effects of D2 depletion? We found that satellite cell specific D2-depletion in resting condition induces their transition from G0 into G_{Alert} while promotes cell proliferation and expansion in regenerative conditions. Reducing TH, induces a break in quiescence and a

transition into G_{Alert} state. The sustained D2-mediated TH activity is then responsible for the maintenance of quiescence in resting muscle. The transition from G0 to G_{Alert} was initially demonstrated in quiescent cells by the action of systemic HGFA released upon muscle injury (12). Here we found that a metabolic decrease in TH intracellular concentration by D2 depletion is sufficient by itself to induce G_{Alert} in absence of systemic cues. Mechanistically, we found that, D2 depletion causes activation of MTOR and S6K and a corresponding reduction in pAMPK (Figure 8C-F). The effects of D2-depletion and corresponding reduction of TH concentration are in agreement with the previously described effects of TH treatment on pAMPK levels in C2C12 myoblasts (37). Interestingly, the molecular gene program triggered by D2-depletion is significantly coincident with the gene program triggered by the Alert condition as previously published (Fig 8J and K), strongly supporting the notion that a large overlapping exists between D2-depletion and the transition into G_{Alert}. Of note, the mechanisms that cause, by systemic cues, entry into G_{Alert} also determine a reduction of D2 levels. The reduced D2 expression level measured in Alerted muscle stem cells (fig 8I) obtained by CTX stimuli represented an important support to the association between G_{Alert} and D2. The molecular mechanisms for that are presently unknow, but it is not unconceivable to hypothesize a potential inhibition of D2 levels by circulating growth factors normally acting as alarmins in the plasma. In regenerative conditions, D2-depletion increases the number of proliferating myoblasts favoring progenitor expansion. However, “reserve experiments” in vitro (Figure 3A-D) and reservoir upon multiple challenges, *in vivo* indicate that D2 action is also required to return quiescence (Figure 6A-K). While we previously demonstrated that in global D2-KO mice sustained satellite cell proliferation is associated with delayed differentiation and muscle repair, our temporally transient pharmacological block of D2-action obtained by rT3 treatment *in vivo* indicate that we could favor expansion of stem cells at early stage of regeneration/wound healing without hampering the subsequent differentiation potential (Figure 12A-G), which ultimately lead to a faster repair of muscle and skin upon injuries. Vice versa, permanent D2-depletion has negative consequences also due to reduced self-renewal as observed under multiple stresses (Figure 6). The capacity of D2-depletion to enhance cell proliferation was confirmed by the engrafting experiments, which showed enhanced engrafting potential of D2-depleted cells vs control. The latter is likely the result of a potentiated expansion of muscle stem cells which– in absence of D2- determine a larger pool of progenitor myoblasts

in mdx-D2KO mice that eventually, with a time delay- differentiate into myotubes. The increased expansion of activated myoblasts pool is likely the explanation for the positive effects observed upon D2-blocking in stem cells in acute regenerative conditions (i.e.in muscle injury and wound healing) as well as in the mdx-D2KO context, where the onset of dystrophy is delayed and the number of Pax7 cells is retained with time respect to control. This result suggests that D2 -depletion is beneficial for the expansion of the progenitor cell pool in both normal and pathological settings. Overall, this study identifies TH-dependent signaling as intracellular metabolic hub responsible for maintenance of quiescence, and for the first time establishes a direct connection between a hormonal signal and the control of quiescence and stemness in solid organ stem cells as well as illustrates their potential therapeutic use in stem cell-based therapies.

6 Materials and methods

6.1 Animals and Procedures

Animals were house and maintained in the animal facility at CEINGE Biotecnologie Avanzate, Naples, Italy. Tg: Pax7-nGFP; $Pax7^{CreER}$ $R26^{mTmG}$ mice were kindly provided by Shahragim Tajbakhsh (Pasteur Institute, Paris, France) (38), Dio2 $^{flox/flox}$ (39), D2-3xFLAG (29), *mdx* (dystrophic muscle) mice (40), global-D2KO (41) were used in this study. Gt (ROSA)26$Sor^{tm1(Notch1)Dam}$/J and C57BL/6 were purchased from The Jackson Laboratory (Stock No: 008159 and 000664 respectively). All mice used for experiments were adults, between 12-16 weeks of age while *mdx* mice used were between 12- 50 weeks of age as indicated. Both sexes were used for experiments as indicated. Animals were genotyped by PCR using tail DNA. Tamoxifen (Sigma Aldrich) was dissolved in corn oil/10% ethanol at a concentration 10mg/ml and was administrated 200µl per mouse for three or five consecutive days by intraperitoneal injection for experiments involving inducible CreERT2. To evaluate in vivo cell proliferation, animals were administrated 10 mg/ml Bromodeoxyuridine (BrdU) (Sigma Aldrich) in drinking water or were injected intraperitoneally with EdU (Sigma Aldrich) at 2.5mg/ml as indicated in the results section. Experiments and animal care were performed in accordance with institutional guidelines. All animal studies were conducted in accordance with the guidelines of the Ministero della Salute and were approved by the Institutional Animal Care and Use Committee (IACUC: 167/2015-PR and 354/2019-PR).

6.2 Cell cultures, reagents

C2C12 were obtained from ATCC. Proliferating cells were cultured in Dulbecco's modified Eagle's medium (DMEM) supplemented with 20% Fetal Bovine Serum (FBS) 2mM glutamine, 50 i.u. penicillin and 50µg/ml streptomycin at 37°C with penicillin/streptomycin. To induce differentiation, cells at 70% confluence were switched from 20% FBS to 2% horse serum (HS) and Dulbecco's modified Eagle's medium supplemented with 10µg/ml insulin and 5µg/ml transferrin.

4.3 FACS-Sorted

Cells were isolated by FACS from Tg: Pax7-nGFP mice as previously described (38). In brief, limb muscles were dissected and minced in ice-cold DMEM. Samples were then incubated with a mix of 0.1% collagenase A , 0.2% Dispase II and 2.5mM $CaCl_2$ for 30 minutes at 37°C in shaking water bath. After digestion DMEM was added to the muscle suspension and filtered, through a 70-µm cell strainers, then spun at 50g for 10 min at 4°C to remove large tissue fragments. The supernatant was collected and washed twice by centrifugation at 600g for 15 min at 4°C. Before fluorescence-activated cell sorting (FACS), the final pellet was resuspended in cold DMEM and 1% penicillin-streptomycin supplemented with 2% FBS, and the cell suspension was filtered through a 40-µm strainer.FACS was performed using FACS Aria IIIu (Becton Dickinson) by gating for GFP fluorescence. MuSCs have been cultured in 1:1 DMEM:MCDB containing 20% serum FBS, 1% penicillin-streptomycin 2% ultroser^{TM}G (PALL-life sciences). Cells were plated on Matrigel (BD Biosciences; catalog #354234) or collected in a lysis buffer for RNA or protein extraction.

To isolate skin stem cells, dorsal skin was removed from mice and treated with trypsin 0.25% over night after removal of adipose tissue. The epidermal layer was separated from derma, chopped and incubated with trypsin 0.25% for 7 minutes to 37°C. After digestion, FBS was added to sample to inactivate trypsin. The cells were filtered with 70µm cell strainer. Immunostaining was performed using APC-anti-mouse CD34 (cod 119310; Biolegend), PE-rat anti human alpha-integrin (cod 555736; BD Pharmingen), upon incubation for 1 hour at room temperature. Fluorescence-activated cell sorting analysis was performed using FACS Aria IIIu (Becton Dickinson).

6.4 Single myofiber isolation and culture

Single myofibers were isolated from the Extensor Digitorum Longus (EDL) muscle and incubated with 0.1% collagenase type I (Sigma Aldrich, cat. #C9891) in DMEM for 60-70 minutes at 37°C. Following enzymatic digestion, mechanical dissociation was performed to release individual myofibres that were then transferred in 60-mm fetal bovine serum (FBS) -coated plates in DMEM/ F12 (50%) supplemented with 20% FBS, 1% penicillin-streptomycin (Gibco). Fibers were fixed at different time points after plating fibers were fixed in 4% PFA for 10 minutes and stained for specific antibody. For experiments with the chemotherapeutic drug AraC (Cytosine ß-D-arabinofuranoside, Sigma Aldrich,

cat. # C1768), myofibers were cultured for 72 hours in medium and then incubated with 100 μM AraC for 48 hours and fixed (day 5).

6.5 Western Blotting

Muscle stem cells freshly isolated from cD2KO or wild type mice were lysed in radioimmunoprecipitation assay (RIPA) buffer (50 mM Tris-Cl [pH 8.0], 200 mM NaCl, 50 mM NaF, 1 mM dithiothreitol, 1 mM Na3VO4, 0.3% IGEPAL, and protease inhibitor cocktail). Cells were boiled at 99°C for 5min and centrifuged for 10min at 300rpm. The samples were loaded in each lane onto 10% SDS-PAGE gels followed by Western Blot. The antibodies used are listed in Table S1 of the supplemental material. Antibody-labeled protein bands were revealed by using the RapidStep enhanced chemiluminescence reagent (ECL Kit) (Millipore, cat. WBKLS0500). The gel images were analyzed using ImageJ software.

6.6 qPCR

Total RNA was extracted from freshly sorted or cultured cells with a Qiagen RNeasy Micro kit according to the manufacturer's instructions (Qiagen, Hilden, Germany) and then reverse-transcribed into cDNA by using VILO reverse transcriptase (Invitrogen Life technologies Ltd) according to the manufacturer's instructions. Quantitative real-time PCR was performed using iQ5 Multicolor Real Time Detector System (BioRad) with SYBR Green Master mix (BioRad). Cyclofilin A gene was used as the housekeeping gene controls for ΔC_T calculations [ΔC_T = (C_T of the target gene) - (C_T of housekeeping genes)]. Primer sequences are detailed in Table S2 of the supplemental material. Fold expression values were calculated using the $2^{-\Delta\Delta CT}$ method, where $\Delta\Delta C_T$ = (ΔC_T of the treatment sample) - (ΔC_T of control samples) (with the control value normalized to 1). Three technical replicates were performed for all qPCR experiments.

6.*7* Chromatin Immunoprecipitation (Chip assay)

Mouse C2C12 myoblasts were cross-linked with 1% formaldehyde in culture medium for 10 min at RT after which cells were scraped into SDS lysis buffer. The cells were further sonicated and diluted for immunoprecipitation with the indicated antibodies. The immunoprecipitates were eluted and de-crosslinked overnight at 65°C. DNA fragments were extracted, and qPCR was performed for

quantification. As negative control, PCR was carried out by using unrelated oligonucleotides, and the presence of equivalent amounts of chromatin in each sample was confirmed by PCR without prior immunoprecipitation (input).

6.8 Immunofluorescence and Histology

Dissected muscles were snap frozen in liquid nitrogen-cooled isopentane, sectioned (7 µm thick) and stained. For immunofluorescent staining, cells or section were fixed with 4% formaldehyde (PFA) and permeabilized in 0.1% Triton X-100, then blocked with 0.5% goat serum and incubated with primary antibody. Alexa Fluor^{TM} 594/647-conjugated secondary antibody was used. Images were acquired with an IX51 Olympus microscope and the Cell*F software. For hematoxylin/eosin staining (H&E), sections were fixed for 15 min and placed in hematoxylin for 5 min followed washed, and 5 min in Eosin. For Oil Red O (Sigma-Aldrich Co. LLC, USA), sections were placed in 60% isopropanol, followed by 75min incubation in 0.5g oil red and 1% of destrin solution in 98% isopropanol; washed in 60% isopropanol then water. The sections were counterstained with Mayer's hematoxylin for 2min. For Sirius Red, sections were fixed with 4% PFA for 10min and stained in Sirius Red solution for 60/90min at room temperature (RT) protected from light. After washing in acidified water, sections were fixed in 100% ethanol and dehydrated in 100% xylene. Sections were mounted with EUKITT.

6.9 Cross Sectional Area (CSA)

The tibialis anterior (TA) muscles were dissected and fixed in isopentane in liquid nitrogen, and sliced into 7µm sections. The cross-sectional area was analyzed and quantified using CellF*Olympus Imaging Software.

6.10 Muscle injury

Animals were anesthetized by a ketaminexylazine cocktail, and 12.5 µl of CTX (60µg/ml *Naja mossambica mossambica*, Sigma-Aldrich) were injected into and along the length of the right tibialis anterior (TA) (Yan et al., 2003) and 25 µl into gastrocnemius muscle. CTX was injected on different day upon tamoxifen (TAM) treatment.

4.11 Transplantation

Freshly isolated MuSCs from $Pax7^{CreERT}$; $D2^{fl/fl}$; $R26^{mTmG}$ vs $Pax7^{CreERT}$; $D2^{+/+}$; $R26^{mT/mG}$ 12 old weeks Tamoxifen treated mice, were isolated using FACS machine and they were counted, washed with PBS resuspended in PBS with 0.1% BSA at a concentration of 1-3x10^4 cells/20 µl. The receivers 8 old weeks *mdx* mice were anaesthetized by a ketaminexylazine cocktail, by intraperitoneal (IP) injection. Donor MuSCs were transplantated into TA receiver mdx mouse for skeletal muscle regeneration. The transplantation was performed slowly injecting 10 µl of the donor cell solution into the TA using a 25µl Hamilton syringe. Each host mouse received transplantation of MuSCs cD2KO into the left TA and MuSCs wt into the right TA. Twenty-one and 40 days after transplantation we frozen TA muscle sections and sections were processed for immunofluorescence. For Transplantation at long time point (40 days post-xenograft), we started treat mice with tacrolimus (anti-rejection drug) in water at 11 days post xenograft.

4.12 Hair follicle cycle

Dorsal back of 3-months-old anesthetized D2KO and control mice were shaved using clamp (43). The mice were harvested after 6 days for the anagen, 10 days for the catagen and 60 days for the telogen analysis and dorsal skin was collected for molecular and histological analysis (44).

6.13 Wound preparation, macroscopic examination and histological analyses

The back fur was shaved and the skin was cleaned with 70% alcohol. The dorsal skin was pulled using forceps and two 8-mm full-thickness skin wounds were created along the midline using a sterile 8 mm circular biopsy punch by pressing through both layers of the skin pull. Skin wound healing was measured every 2-3 days by anesthetizing the animals and imaging the wounded area. Excisional, full-thickness skin wounds were aseptically made on the dorsal skin by picking up a fold skin at the midline and using a sterile, disposable biopsy punch with a diameter of 8 mm to punch through the two layers of skin. In this manner, two wounds were made on each side of the midline at the same time. Each wound site was digitally photographed using the Nikon FX-35A at the indicated time intervals, and wound areas were determined on photographs using CellF*. Changes in wound areas were expressed as the percentage of the initial wound areas.

6.14 EdU incorporation assay in vivo

EdU (2.5 mg/ml) was injected to animals contemporary to TAM induction, as indicated in the figures. EdU was detected using the Click-It kit (Invitrogen) according to the manufacturer's instructions on MuSCs by FACS. Data on EdU incorporation are presented as the percentage of EdU^+ *versus* total cells (measured by DAPI).

6.15 Cell Size

The cell size of MuSCs was evaluated by the analysis of the forward scatter (FSC) by FACS.

6.16 Mitochondrial DNA

DNA was extracted from about 50,000 freshly FACS- isolated MuSCs using the QIAamp DNA Micro Kit (Qiagen) per the manufacturer's instructions. mtDNA was quantified using primers amplifying the cytochrome B region on mtDNA relative to the β-globin region on genomic DNA by RT-qPCR.

6.17 Magnetic Sorting of Muscle Stem Cells

In brief, muscle dissection was done with a scalpel by removing the tissue from the bone in DMEM. Muscles were then chopped and digested with 0.1% collagenase A and 0.2% dispase for 30 minutes at 37°C. The collagenase/dispase solution was added to continue the digestion until the process was completely terminated and muscle totally digested. The dissociated single cells were filtered through 70-micron strainer and pelleted by centrifugation at 400g for 5 mins at 4°C. Cells were washed twice with DMEM and proceed with MACS Cell Separation. Muscle stem cells were isolated according to the protocol of the Satellite Cell Isolation Kit (MiltenyiBiotec, 130-104-268). For further purification, MuSCs have been labeled with Anti-Integrin α-7 MicroBeads (MiltenyiBiotec, 130-104-261) and isolated using LS Columns and a MACS Separator. The flow-through fraction was discarded, and MuSCs were collected in the eluted fraction.

6.18 Rosalind™ RNA-seq Methods

Data was analyzed by Rosalind (https://rosalind.onramp.bio/), with a HyperScale architecture developed by OnRampBioInformatics, Inc. (San Diego, CA).

Individual sample counts were normalized via Relative Log Expression (RLE) using DESeq2 R library.

6.19 rT3 administration

Mice (C56BL6 mice) were administrated 2 µg/ml of rT3 (Sigma Aldrich #T0281) in drinking water or PBS as control for 10 consecutive days.

6.20 Statistical Analysis

Significant differences were determined using ANOVA, and Student's t test, for independent samples, with $p < 0.05$ considered as statically significant. All statistics and graphics were performed using GraphPad Prism7 and appear in more detail in the SI Appendix, S20. In all figures, error bars represent the SEM. A value of $p < 0.05$ was considered significant (*P < 0.05; **P < 0.01; ***P < 0.001).

REFERENCES

1. Brack AS, and Rando TA. Tissue-specific stem cells: lessons from the skeletal muscle satellite cell. *Cell stem cell.* 2012;10(5):504-14.
2. Dhawan J, and Rando TA. Stem cells in postnatal myogenesis: molecular mechanisms of satellite cell quiescence, activation and replenishment. *Trends in cell biology.* 2005;15(12):666-73.
3. Rudnicki MA, Le Grand F, McKinnell I, and Kuang S. The molecular regulation of muscle stem cell function. *Cold Spring Harbor symposia on quantitative biology.* 2008;73(323-31.
4. Tumbar T, Guasch G, Greco V, Blanpain C, Lowry WE, Rendl M, and Fuchs E. Defining the epithelial stem cell niche in skin. *Science.* 2004;303(5656):359-63.
5. Fuchs E, Tumbar T, and Guasch G. Socializing with the neighbors: stem cells and their niche. *Cell.* 2004;116(6):769-78.
6. Yin H, Price F, and Rudnicki MA. Satellite cells and the muscle stem cell niche. *Physiological reviews.* 2013;93(1):23-67.
7. Abou-Khalil R, and Brack AS. Muscle stem cells and reversible quiescence: the role of sprouty. *Cell cycle.* 2010;9(13):2575-80.
8. Bjornson CR, Cheung TH, Liu L, Tripathi PV, Steeper KM, and Rando TA. Notch signaling is necessary to maintain quiescence in adult muscle stem cells. *Stem cells.* 2012;30(2):232-42.
9. Wen Y, Bi P, Liu W, Asakura A, Keller C, and Kuang S. Constitutive Notch activation upregulates Pax7 and promotes the self-renewal of skeletal muscle satellite cells. *Molecular and cellular biology.* 2012;32(12):2300-11.
10. Fujimaki S, Seko D, Kitajima Y, Yoshioka K, Tsuchiya Y, Masuda S, and Ono Y. Notch1 and Notch2 Coordinately Regulate Stem Cell Function in the Quiescent and Activated States of Muscle Satellite Cells. *Stem cells.* 2018;36(2):278-85.
11. Rodgers JT, King KY, Brett JO, Cromie MJ, Charville GW, Maguire KK, Brunson C, Mastey N, Liu L, Tsai CR, et al. mTORC1 controls the adaptive transition of quiescent stem cells from G0 to G(Alert). *Nature.* 2014;510(7505):393-6.
12. Rodgers JT, Schroeder MD, Ma C, and Rando TA. HGFA Is an Injury-Regulated Systemic Factor that Induces the Transition of Stem Cells into GAlert. *Cell reports.* 2017;19(3):479-86.
13. Gereben B, Zavacki AM, Ribich S, Kim BW, Huang SA, Simonides WS, Zeold A, and Bianco AC. Cellular and molecular basis of deiodinase-regulated thyroid hormone signaling. *Endocrine reviews.* 2008;29(7):898-938.

14. Ortiga-Carvalho TM, Sidhaye AR, and Wondisford FE. Thyroid hormone receptors and resistance to thyroid hormone disorders. *Nature reviews Endocrinology.* 2014;10(10):582-91.
15. Bernal J, Guadano-Ferraz A, and Morte B. Thyroid hormone transporters-functions and clinical implications. *Nature reviews Endocrinology.* 2015;11(12):690.
16. Dentice M, Marsili A, Zavacki A, Larsen PR, and Salvatore D. The deiodinases and the control of intracellular thyroid hormone signaling during cellular differentiation. *Biochimica et biophysica acta.* 2013;1830(7):3937-45.
17. Ambrosio R, De Stefano MA, Di Girolamo D, and Salvatore D. Thyroid hormone signaling and deiodinase actions in muscle stem/progenitor cells. *Molecular and cellular endocrinology.* 2017;459(79-83.
18. Dentice M, Marsili A, Ambrosio R, Guardiola O, Sibilio A, Paik JH, Minchiotti G, DePinho RA, Fenzi G, Larsen PR, et al. The FoxO3/type 2 deiodinase pathway is required for normal mouse myogenesis and muscle regeneration. *The Journal of clinical investigation.* 2010;120(11):4021-30.
19. Bianco AC, Salvatore D, Gereben B, Berry MJ, and Larsen PR. Biochemistry, cellular and molecular biology, and physiological roles of the iodothyronine selenodeiodinases. *Endocrine reviews.* 2002;23(1):38-89.
20. Cheng SY. Thyroid hormone receptor mutations and disease: beyond thyroid hormone resistance. *Trends in endocrinology and metabolism: TEM.* 2005;16(4):176-82.
21. Darras VM, Houbrechts AM, and Van Herck SL. Intracellular thyroid hormone metabolism as a local regulator of nuclear thyroid hormone receptor-mediated impact on vertebrate development. *Biochimica et biophysica acta.* 2015;1849(2):130-41.
22. Astapova I. Role of co-regulators in metabolic and transcriptional actions of thyroid hormone. *Journal of molecular endocrinology.* 2016;56(3):73-97.
23. Dentice M, Ambrosio R, Damiano V, Sibilio A, Luongo C, Guardiola O, Yennek S, Zordan P, Minchiotti G, Colao A, et al. Intracellular inactivation of thyroid hormone is a survival mechanism for muscle stem cell proliferation and lineage progression. *Cell metabolism.* 2014;20(6):1038-48.
24. Catalano V, Dentice M, Ambrosio R, Luongo C, Carollo R, Benfante A, Todaro M, Stassi G, and Salvatore D. Activated Thyroid Hormone Promotes Differentiation and Chemotherapeutic Sensitization of Colorectal Cancer Stem Cells by Regulating Wnt and BMP4 Signaling. *Cancer research.* 2016;76(5):1237-44.

25. Worton RG, Duff C, Sylvester JE, Schmickel RD, and Willard HF. Duchenne muscular dystrophy involving translocation of the dmd gene next to ribosomal RNA genes. *Science.* 1984;224(4656):1447-9.
26. Hoffman EP, Brown RH, Jr., and Kunkel LM. Dystrophin: the protein product of the Duchenne muscular dystrophy locus. *Cell.* 1987;51(6):919-28.
27. McIntosh LM, Pernitsky AN, and Anderson JE. The effects of altered metabolism (hypothyroidism) on muscle repair in the mdx dystrophic mouse. *Muscle & nerve.* 1994;17(4):444-53.
28. Izumo S, Nadal-Ginard B, and Mahdavi V. All members of the MHC multigene family respond to thyroid hormone in a highly tissue-specific manner. *Science.* 1986;231(4738):597-600.
29. Castagna MG, Dentice M, Cantara S, Ambrosio R, Maino F, Porcelli T, Marzocchi C, Garbi C, Pacini F, and Salvatore D. DIO2 Thr92Ala Reduces Deiodinase-2 Activity and Serum-T3 Levels in Thyroid-Deficient Patients. *The Journal of clinical endocrinology and metabolism.* 2017;102(5):1623-30.
30. Seale P, Sabourin LA, Girgis-Gabardo A, Mansouri A, Gruss P, and Rudnicki MA. Pax7 is required for the specification of myogenic satellite cells. *Cell.* 2000;102(6):777-86.
31. Yoshida N, Yoshida S, Koishi K, Masuda K, and Nabeshima Y. Cell heterogeneity upon myogenic differentiation: down-regulation of MyoD and Myf-5 generates 'reserve cells'. *Journal of cell science.* 1998;111 (Pt 6)(769-79.
32. Collins CA, Olsen I, Zammit PS, Heslop L, Petrie A, Partridge TA, and Morgan JE. Stem cell function, self-renewal, and behavioral heterogeneity of cells from the adult muscle satellite cell niche. *Cell.* 2005;122(2):289-301.
33. Zammit PS, Golding JP, Nagata Y, Hudon V, Partridge TA, and Beauchamp JR. Muscle satellite cells adopt divergent fates: a mechanism for self-renewal? *The Journal of cell biology.* 2004;166(3):347-57.
34. Ontell M. Muscular dystrophy and muscle regeneration. *Human pathology.* 1986;17(7):673-82.
35. Bianchi A, Mozzetta C, Pegoli G, Lucini F, Valsoni S, Rosti V, Petrini C, Cortesi A, Gregoretti F, Antonelli L, et al. Dysfunctional polycomb transcriptional repression contributes to lamin A/C-dependent muscular dystrophy. *The Journal of clinical investigation.* 2020;130(5):2408-21.
36. Garcia-Serrano L, Gomez-Ferreria MA, Contreras-Jurado C, Segrelles C, Paramio JM, and Aranda A. The thyroid hormone receptors modulate the skin response to retinoids. *PloS one.* 2011;6(8):e23825.

37. Yamauchi M, Kambe F, Cao X, Lu X, Kozaki Y, Oiso Y, and Seo H. Thyroid hormone activates adenosine 5'-monophosphate-activated protein kinase via intracellular calcium mobilization and activation of calcium/calmodulin-dependent protein kinase kinase-beta. *Molecular endocrinology.* 2008;22(4):893-903.
38. Rocheteau P, Gayraud-Morel B, Siegl-Cachedenier I, Blasco MA, and Tajbakhsh S. A subpopulation of adult skeletal muscle stem cells retains all template DNA strands after cell division. *Cell.* 2012;148(1-2):112-25.
39. Luongo C, Martin C, Vella K, Marsili A, Ambrosio R, Dentice M, Harney JW, Salvatore D, Zavacki AM, and Larsen PR. The selective loss of the type 2 iodothyronine deiodinase in mouse thyrotrophs increases basal TSH but blunts the thyrotropin response to hypothyroidism. *Endocrinology.* 2015;156(2):745-54.
40. Anderson JE, Liu L, Kardami E, and Murphy LJ. The pituitary-muscle axis in mdx dystrophic mice. *Journal of the neurological sciences.* 1994;123(1-2):80-7.
41. Christoffolete MA, Arrojo e Drigo R, Gazoni F, Tente SM, Goncalves V, Amorim BS, Larsen PR, Bianco AC, and Zavacki AM. Mice with impaired extrathyroidal thyroxine to 3,5,3'-triiodothyronine conversion maintain normal serum 3,5,3'-triiodothyronine concentrations. *Endocrinology.* 2007;148(3):954-60.
42. Yan Z, Choi S, Liu X, Zhang M, Schageman JJ, Lee SY, Hart R, Lin L, Thurmond FA, and Williams RS. Highly coordinated gene regulation in mouse skeletal muscle regeneration. *The Journal of biological chemistry.* 2003;278(10):8826-36.
43. Plikus MV, Mayer JA, de la Cruz D, Baker RE, Maini PK, Maxson R, and Chuong CM. Cyclic dermal BMP signalling regulates stem cell activation during hair regeneration. *Nature.* 2008;451(7176):340-4.
44. Stenn KS, and Paus R. Controls of hair follicle cycling. *Physiological reviews.* 2001;81(1):449-94.